Exxon Valdez Oil Spill
Long-Term Herring Research and Monitoring Program Final Report

Genomic mechanisms that underlie lack of recovery of Prince William Sound herring following the 1990's collapse

Exxon Valdez Oil Spill Trustee Council Project 21170115
Final Report

Andrew Whitehead

Department of Environmental Toxicology, University of California Davis
1 Shields Avenue
Davis, CA 95616

March 2023

Exxon Valdez Oil Spill
Long-Term Herring Research and Monitoring Program Final Report

Genomic mechanisms that underlie lack of recovery of Prince William Sound herring following the 1990's collapse

Exxon Valdez Oil Spill Trustee Council Project 21170115
Final Report

Andrew Whitehead

Department of Environmental Toxicology, University of California Davis
1 Shields Avenue
Davis, CA 95616

March 2023

Genomic mechanisms that underlie lack of recovery of Prince William Sound herring following the 1990's collapse

Exxon Valdez Oil Spill Trustee Council Project 21170115
Final Report

Study History: This project was initiated in 2017 to investigate the effects of oil exposure on genetic change through time on Pacific herring and its potential role in the lack of recovery of herring. Annual reports for 2017 - 2020 contributed to this final report. The peer reviewed publication Oziolor et al. (2019) contributed to this final report.

Abstract: The causes of the collapse of Prince William Sound Pacific herring are controversial, and the reasons for the lack of recovery remain a mystery. We interrogated genome structure and function of Prince William Sound fish, in comparison to other populations, to test hypotheses about the causes and consequences of the collapse. Exposures to very low concentrations of crude oil induced cardiac malformations in developing herring, where fish from Prince William Sound and Sitka Sound were equally sensitive but more sensitive than fish from Puget Sound. Transcriptomics revealed the molecular mechanisms underlying these treatment effects. Populations were equally sensitive to viral hemorrhagic septicemia virus exposure. Brief oil exposures to larval fish caused reduced sensitivity to virus in later life. Whole genome sequencing of ~60 individuals from each of three populations (Prince William Sound, Sitka Sound, Togiak Bay) and four time points (1991-2017), and three other populations (Central British Columbia, Puget Sound, San Francisco Bay in 2017) showed that Togiak Bay populations are very distinct from all others. Large chromosomal inversions distinguish the San Francisco Bay population. Signatures of polygenic selection through time are detected only in the Prince William Sound population, suggesting that environmental changes over the past three decades that are specific to Prince William Sound have impacted fitness in that population.

Key words: Adaptation, crude oil exposure, ecotoxicology, evolution, population genomics, population variation, transcriptomics, viral hemorrhagic septicemia virus, virus

Project Data: As per common practice in this field, population genomics data (fasta format) have been uploaded to the National Center for Biotechnology Information (NCBI) for long-term archival but have not yet been made public – we will make these data public once manuscripts are submitted for peer review. RNA-seq data (fasta format) are also uploaded to NCBI. Once these data are ready for publication, we will create a project page at the European Bioinformatics Institute (EBI) BioStudies that will include links to raw data at NCBI, and will also house variant call files for the population genomics data and matrices of read counts for the RNA-seq data. The EBI site will also house data from animal challenge experiments. All custom bioinformatics scripts are archived at GitHub, and will be linked through the EBI BioStudies project site. We have archived all of our scripting for population genomics work and transcriptomics work on dedicated GitHub pages which are durable archives, and will be made publicly available once

manuscripts are in review. Publications will also be linked through the BioStudies project site. The databases described above are designed to accommodate the types of data that we need to make public, and they are durable, and they are standard practice for our research field. Once these data are public, DOIs will be generated and made available through the Gulf of Alaska Data Portal.

The data custodian for the Gulf of Alaska Data Portal is Carol Janzen, Director of Operations and Development, Alaska Ocean Observing System, 1007 W. 3rd Ave. #100, Anchorage, AK 99501, 907-644-6703. janzen@aoos.org.

Data are archived by Axiom Data Science, a Tetra Tech Company, 1016 W. 6th Ave., Anchorage, AK 99501.

Citation:

Whitehead, A. 2023. Genomic mechanisms that underlie lack of recovery of Prince William Sound herring following the 1990's collapse. Long-Term Herring Research and Monitoring Program Final Report, (*Exxon Valdez* Oil Spill Trustee Council Project 21170115), *Exxon Valdez* Oil Spill Trustee Council, Anchorage, Alaska.

TABLE OF CONTENTS

LIST OF TABLES

LIST OF FIGURES

Genomic mechanisms that underlie lack of recovery of Prince William Sound herring following the 1990's collapse

EXECUTIVE SUMMARY

The Pacific herring (*Clupea pallasii*) population in Prince William Sound (PWS), Alaska, experienced a severe collapse in 1992-1993 that is exceptional among herring populations world-wide, and has yet to recover. In the spring of 1989, the *Exxon Valdez* oil tanker ran aground and spilled 11 million gallons of crude oil into PWS. The timing of this catastrophic event and its devastating impact on local wildlife initially suggested a link between oil exposure and herring population collapse. However, the extent to which the 1989 oil spill contributed to the 1993 collapse remains controversial and the lack of recovery after 27 years is largely unexplained.

Oil can be toxic at extremely low concentrations to developing fish embryos including herring. Therefore, given the extent of EVOS oiling, and its coincidence with spawning season, PWS fish were exposed to toxic oil in 1989 and 1990 over a large area. Furthermore, pathogen exposures likely played a significant role in the PWS collapse, suggesting potential interactions between oil and virus exposures. Exposure to the EVOS may have contributed to the herring collapse either through direct delayed toxicity, through the interactive effects of oil and pathogen exposures, or through evolved tolerance to toxicity that came at the cost of compromised immune function. Alternatively, the PWS herring population collapse could have been unrelated to the oil spill, but erosion of genetic diversity associated with the collapse could compromise recovery, compromise resilience to pathogens, or may limit the ability of the population to adapt to future environmental change. Knowledge of the dynamics of population genetic change through time will help inform management activities for Pacific herring, and could contribute novel considerations for the complexity through which populations respond to oil spills.

We proposed the following hypotheses: 1) Exposure to contaminating oil during 1989 and afterwards selected for genetic variants with impaired aryl hydrocarbon receptor function in developing embryos. Alternatively (or in addition), exposure to oil in 1989 and perhaps to lingering oil in subsequent years impaired immune function. 2) The frequency of individuals with impaired immune function increased within the PWS population. 3) By 1993, fish from the PWS 1989 year class were recruited into the fishery, contributing fish with impaired resilience to pathogens, enabling an epizootic, that contributed to the population collapse. 4) Recovery is slow in PWS because compensatory adaptations for immune function is slow, possibly because the collapse significantly eroded genetic diversity available for subsequent natural selection on immune system genes. We designed our proposed experiments and contrasts to test this set of hypotheses, as well as to test complementary and alternative hypotheses.

We conducted retrospective population genomics studies, and exposure studies on developing Pacific herring from multiple populations. Population genetics studies were designed to detect the influence of recent natural selection in Alaska populations, which would be biological

markers of recent environmental changes that imposed challenges to health, performance, reproduction, and survival. We used new, sophisticated, and sensitive computational tools to detect these markers, as we retrospectively tracked genetic change through time. Exposure studies used fish from multiple populations, including PWS, Sitka Sound (AK), and Puget Sound (WA). We chose these three populations so that comparisons between them could reveal the influence of natural selection. We performed low-dose oil exposure experiments during embryogenesis, measured toxicity (developmental deformities) and genome-wide gene expression, and compared those between populations. Gene expression data offer deep insight into the molecular and cellular mechanisms through which oil prompts defensive responses and causes toxicity, and mechanisms that underlie population differences. From each population we also tested whether early-life oil exposure affected sensitivity to later-life exposure to virus. We also tested whether populations differed in their sensitivity to virus, and whether any oil effect on virus sensitivity varied between populations.

Objectives

Aim 1 objective: Generate insight into the genetic changes that contributed to, or resulted from, the Pacific herring collapse in PWS. By characterizing patterns of genetic change through time in PWS fish, and fish from reference populations, we can both test and generate hypotheses about the causes and consequences of Pacific herring population crash following the EVOS. Evidence for the influence of natural selection or contraction of allelic diversity in PWS could help guide restoration efforts.

Aim 2 objective: Test whether early-life exposure to oil compromises the ability of older fish to mount an effective immune response to common pathogens endemic to PWS herring. Much research has focused on the direct effects of crude oil, including low concentrations that may persist as lingering oil for long periods of time on fish development. However, less is known of how oil may interact with other stressors, including those normally encountered by natural populations such as exposure to pathogens and disease.

Aim 3 objective: Test whether the PWS population varies from other populations in their ability to tolerate oil exposure during early life and/or to mount a robust protective immune response to viral pathogen. The comparative studies proposed here may provide key insights into how recent ecological and evolutionary processes have shaped population differences in response to environmental stress. These studies seek to reveal the reasons for population differences in sensitivity to oil toxicity and disease.

Methods

For the population genetics objectives, we sampled tissue from PWS herring that were collected in1991, 1996, 2006/2007, and 2017. We sequenced whole genomes from each of ~60 individual fish per year. We then explored how the genetic attributes of the population changed over time, immediately after the EVOS but before the collapse, after the collapse, and for two decades following the collapse during which time there has been little recovery. To distinguish the

influence of these environmental impacts from other factors, we collected similar data from two other Alaska populations of Pacific herring that did not experience oil spills, disease epidemics, or population collapses (Togiak Bay and Sitka Sound). We scanned genome sequences for the impacts of natural selection and population decline across successive time periods. Furthermore, we collected similar data from 2017 for three other populations that span the geographic range of Pacific herring in North America (Central British Columbia, Canada; Puget Sound, Washington; and San Francisco Bay, California), which allowed us to test for the ecological and evolutionary forces that have shaped genetic variation through space and time in this important species.

Exposure experiments included fish from multiple populations, so that we could test for evolved differences in Pacific herring sensitivity to oil and virus exposures. We included fish from PWS, Sitka Sound, and Puget Sound. We exposed embryos to a range of very low concentrations of oil. These exposures captured the range of concentrations that Pacific herring were exposed to in PWS during the 1989 and 1990 spawning seasons. We tested whether this range of concentrations impacted fish development, with particular focus on the heart, cardiovascular system, and immune system. We collected gene expression data to offer deep insight into the molecular and cellular process that are affected by these exposures. After exposure during embryo development, we transferred these fish to clean water and raised them for many months until they had matured to juvenile stage, at which time their immune system is fully developed. We then challenged fish with virus. We compared virus sensitivity responses (mortality) between fish that had been exposed to oil when they were embryos to those that had not been exposed to oil. This was to test whether exposure to oil during a brief period of very early development impaired the later-life function of the immune system. Since much of the immune system matures after fish have hatched, we also performed oil exposures on larval fish to test for impacts on immune development and function. We repeated all of these experiments on fish from two additional populations – Sitka Sound and Puget Sound. Comparisons between populations allowed us to test hypotheses about how different ecological, environmental, and evolutionary processes have shaped Pacific herring sensitivity to oil and virus.

Results and Discussion

The extremely deep and rich population genetics data that we generated revealed much about population variation in space and time. The Togiak Bay population from the Bering Sea was the most genetically unique. This indicates little genetic exchange around the Alaska Peninsula, either because of limited migration, or because distinct environments have favored distinct genetic types (through natural selection). The California population was also unique, especially in very discrete portions of their genome where large sections of several chromosome arms are reversed in their orientation. Such large structural mutations tend to harbor genes that are important for local adaptations. Ongoing analyses are examining the identity of genes in those regions, where preliminary analyses indicate their importance for governing the seasonal timing of spawning in response to temperature. Analyses of genetic change through time in Alaskan populations indicates that the PWS population has experienced natural selection over the past

three decades following the EVOS, epidemic, and collapse, whereas the Sitka Sound and Togiak Bay populations have not. Moreover, the regions of the genome subject to the pressures of natural selection are not the same between successive time periods. This indicates that the environment has been changing over time, such that genes that affect fitness in one time period are different from those in another. In other words, it appears that selective regimes have been shifting over time. This is consistent with the massive changes in the PWS environment that have unfolded over the past three decades. Ongoing analyses are examining the identity of genes in these important regions of the genome. Preliminary results indicate that genes involved in innate immune responses to virus have been important for fitness in the past three decades. This is consistent with the PWS population evolving in response to viral hemorrhagic septicemia virus (VHSV), but additional confirmation is required.

Exposure experiments provide deep insights into the mechanisms whereby extremely low doses of oil cause toxicity during development. Our lowest doses – in the parts-per-trillion range – were sufficient to initiate molecular defensive responses. Slightly higher doses, including those that were commonly observed during the EVOS in PWS in 1989 and 1990, were sufficient to cause developmental deformities, especially in the heart. Exposures during embryo development did not appear to affect later-life (juvenile) sensitivity to virus exposure, but oil exposures after hatching during mid-larval development did. Since most immune system genes are not turning on until after hatch, and later-life responses to virus are affected by brief oil exposures soon after hatch but not pre-hatch, this indicates that exposure during some periods of immune system maturation perturbs immune system function. And this perturbation persists to affect immune function much later in life. Additional experiments are needed to clearly identify the windows of development during early life when Pacific herring are vulnerable to the impacts of oil on immune system development and function. This is critically important for predicting ecological consequences of oil exposures in Pacific herring and other fish species.

Populations of Pacific herring varied in their sensitivity to embryonic oil exposure but did not vary in their sensitivity to virus. The two Alaska populations were equally sensitive to the developmental impacts of oil, and they were both more sensitive than the Puget Sound population. It required a higher dose of oil to cause cardiac defects in Puget Sound fish than Alaskan fish. The difference in sensitivity in Puget Sound fish is partially accounted for by differences in their ability to accumulate and metabolize various components of oil during early development. But even at similar body levels of oil, Puget Sound fish are less sensitive, indicating that their differences extends beyond metabolism to include reduced sensitivity to the developmental disruptions caused by oil. The ecological and evolutionary reasons for the difference between Puget Sound and Alaska fish are unknown. Perhaps historical and contemporary exposures to urban chemicals in Puget Sound are responsible? Our experiments were designed to detect the ecological and evolutionary reasons for differences between PWS fish and others. Therefore, in order to discover the ecological and evolutionary reasons why Puget Sound fish differ in their sensitivity to oil, we require new experiments.

INTRODUCTION

The Pacific herring (*Clupea pallasii*) population in Prince William Sound (PWS), Alaska experienced a severe collapse that is exceptional among herring populations world-wide (Trochta et al. 2020). The fishery declined from approximately 133 thousand metric tons of spawning biomass in 1988 to 30 thousand metric tons by 1993 and has yet to recover. In the spring of 1989, the *Exxon Valdez* spilled 11 million gallons of crude oil into PWS. The timing of this catastrophic event and its devastating impact on local wildlife initially suggested a link between oil exposure and herring population collapse. Indeed, 50% of the egg biomass deposited in 1989 was within the trajectory of spilled oil (Carls et al. 2002) and the contribution of the 1989 year class to the 1993 spawning population was 25% of that forecast (Marty et al. 2003). However, after decades of research, the extent to which the oil spill contributed to the 1993 collapse remains controversial and the lack of recovery after 27 years is largely unexplained (Pearson et al. 1999, Thorne and Thomas 2008, Marty et al. 2010).

In the decades following the *Exxon Valdez* oil spill (EVOS), it has become increasingly apparent that oil can be toxic at extremely low concentrations to developing fish embryos including herring (Incardona et al. 2015), where some toxic phenotypes may be apparent during embryogenesis but some are delayed until later in life (Hicken et al. 2011). Therefore, acute and lingering oil impairs fitness and may have acted as an insidious selective force within exposed populations. Much nearshore herring spawning habitat was oiled following the EVOS, and oiling coincided with herring spawning (Carls et al. 2002). In subsequent years, lingering oil, which accumulated in nearshore environments (Short et al. 2004, 2006, 2007) and was bioavailable (Fukuyama et al. 2000), may have contributed to impacts in subsequent year classes of developing herring in PWS. These exposures may have contributed to the herring collapse either through direct toxicity, through the interactive effects of oil and pathogen exposures, or through evolved changes that came at the cost of compromised immune function. Alternatively, the PWS herring population collapse could have been unrelated to the oil spill, but erosion of genetic diversity associated with the collapse could have compromised recovery, compromised resilience to pathogens, or may limit the ability of the population to adapt to future environmental change. Knowledge of the dynamics of population genetic change through time will help inform management activities for Pacific herring, and could contribute novel considerations for the complexity through which populations respond to oil spills or other anthropogenic stressors including climate change.

We posit that contaminating oil in 1989, and perhaps lingering oil in subsequent years, acted as a selective agent on developing herring, the consequences of which may have contributed to their subsequent decline and/or lack of recovery. Support for this hypothesis emerges from our discoveries about how exposure to pollutants may drive genetic change in populations of Atlantic killifish (*Fundulus heteroclitus*) (Reid et al. 2016) – a forage fish with very large population sizes. Some populations of killifish have rapidly evolved within an environment contaminated with creosote, which is chemically and toxicologically similar to crude oil.

Creosote pollution acted as a strong selective agent, primarily for survivorship during embryogenesis. Favored were genetic variants that affected the activation and function of the aryl hydrocarbon receptor (AHR) signaling pathway. Normal AHR signaling interacts with immune system signaling, such that evolved alterations in AHR function could come at the cost of normal immune system function. Indeed, in killifish populations we find evidence for subsequent selection on immune system genes, which supports this prediction. These discoveries were achieved through population genomics and comparative transcriptomics and physiological analyses, which are similar to those that we conducted for Pacific herring.

Given these findings in Atlantic killifish, and more generally that pollutants can act as powerful selective agents (Monosson 2012), that evolutionary genetic change can occur very rapidly (Hendry et al. 2008), that rapid adaptation often incurs physiological or life history costs (Gassmann et al. 2009, Hochmuth et al. 2015, Qi et al. 2016), that crude oil can interact with immune function (Reynaud and Deschaux 2006), and that crude oil impairs herring development at extremely low concentrations (Incardona et al. 2015), we posit the following: 1) Exposure to contaminating oil during 1989 (and perhaps to lingering oil in subsequent years) selected for genetic variants with altered AHR function in developing embryos. Alternatively (or in addition), exposure to oil in 1989 and perhaps to lingering oil in subsequent years impaired immune function. 2) The frequency of individuals with impaired immune function increased within the PWS population. 3) By 1993, fish from the PWS 1989 year class were recruited into the fishery, contributing fish with impaired resilience to pathogens, enabling an epizootic, that contributed to the population collapse. 4) Recovery is slow in PWS because compensatory adaptations for immune function is slow, possibly because the collapse significantly eroded genetic diversity available for subsequent natural selection on immune system genes. We design our proposed experiments and contrasts to test this set of hypotheses, as well as to test complementary and alternative hypotheses.

We conducted retrospective population genomics studies, and exposure studies on developing Pacific herring from multiple populations. Population genetics studies were designed to detect signatures of recent natural selection in Alaska populations. We contrasted genetic change through time in the PWS population with genetic change through time in two other Alaska populations that did not experience an oil spill, epizootic, or population collapse – from Togiak Bay (TB) and from Sitka Sound (SS). Most current methods of detecting genetic signatures of natural selection are sensitive when selection acts on few genes of large effect – when the genetic basis of adaptive phenotypic change is simple. However, many phenotypic traits are highly polygenic, where standard methods are insensitive for detecting the influence of natural selection at the genetic level. Considering that variation in sensitivity to crude oil and disease may be highly polygenic, we leveraged very recent computational methods that examine covariance in allele frequency change through time. Temporal patterns of subtle allele frequency changes can be used distinguish the influence of selection from random neutral drift, and when examined at the whole-genome scale can detect the influence of polygenic selection across the time scale of

interest (Buffalo and Coop 2019). These methods, developed by our collaborator Vince Buffalo (University of California Berkeley), represent the state-of-the-science for detecting the influence of recent polygenic selection.

Exposure studies used fish from multiple populations, including from PWS, SS, and Puget Sound, Washington We chose these three populations so that comparisons between them could reveal evolved differences in their response to oil and virus exposures, where particular patterns of population variation could distinguish the influence of adaptation from random neutral drift. For example, if random neutral drift were responsible for population differences, then we would expect that the two Alaska populations to be most similar, and the Washington population to be distinct. In contrast, if natural selection from historical exposure to oil or virus had impacted the PWS population, then we would expect PWS fish to be most distinct compared to the SS and Washington populations. We performed low-dose oil exposure experiments during embryogenesis, measured toxicity (developmental deformities) and genome-wide gene expression, and compared those between populations. From each population we also took fish that had been exposed to oil during embryogenesis and no-oil controls, raised them in clean water for many months until juvenile stage, and then exposed them to viral hemorrhagic septicemia virus (VHSV). We tested whether early-life oil exposure affected sensitivity to later-life exposure to virus. We also tested whether populations differed in their sensitivity to virus, and whether any oil effects on virus sensitivity varied between populations.

OBJECTIVES

Aim 1 objective

Generate insight into the genetic changes that contributed to, or resulted from, the Pacific herring collapse in PWS. Over the past two decades it has become increasingly appreciated that population genetic change can happen over very short time scales, including adaptive evolution and changes in genetic diversity. Population genetic characteristics (e.g., allelic diversity, signatures of selection) can illuminate historical processes, can indicate phenotypic attributes that matter for contemporary environments, and can influence the future evolutionary trajectory of populations. By characterizing patterns of genetic change through time in PWS fish, and reference population fish, we can both test and generate hypotheses about the causes and consequences of the Pacific herring population crash that followed the EVOS. Evidence uncovered for natural selection or contraction of allelic diversity in PWS could help guide restoration efforts.

Aim 2 objective

Test whether early-life exposure to oil compromises the ability of later life stages to mount an effective immune response to common pathogens endemic to PWS herring. Much research has focused on the direct effects of crude oil, including low concentrations that may persist as lingering oil for long periods of time, on fish development (e.g., Cherr et al. 2017). However less

is known about how oil may interact with other stressors (Whitehead 2013), including those normally encountered by natural populations such as pathogens and disease.

Aim 3 objective

Test whether the PWS population varies from other populations in their ability to tolerate oil exposure during early life and/or to mount a robust protective immune response to viral pathogen. 21st century toxicology and public health science has been revealing importance of genetic variation in determining individual and population variation in sensitivity to environmental toxicants and disease (National Research Council 2007). 21st century evolutionary biology is recognizing how swiftly genetic characteristics may evolve within populations (Hendry et al. 2008, Alberti 2015), especially those in human-altered environments. The comparative studies proposed here will provide key insights into how recent eco/evolutionary dynamics have shaped population differences in response to environmental stress, and therefore provide a mechanistic basis for understanding variation in contemporary population health.

This research is important because the causes of the Pacific herring collapse in PWS, and reasons for lack of recovery, remain unresolved. Much information about individual and population characteristics, and historical demographic processes, is archived within the genome. Laboratory experiments that compare physiological sensitivities (and underlying molecular mechanisms) between populations, coupled with analysis of population genetic change through space and time, are powerful approaches for shedding light on the historical phenomena the have influenced the evolutionary and demographic trajectories of populations.

METHODS

Aim 1

Experimental design and sample collection

Adult tissues were collected from ~60 fish per population per time point (Table 1). For Alaska populations tissues were collected across time, including 1991, 1996, 2006, and 2017 from TB (Bering Sea), 1991, 1996, 2007, and 2017 from PWS (Gulf of Alaska), and 1996, 2006, and 2017 from SS (Gulf of Alaska). Tissues from populations outside of Alaska (British Columbia, Washington, California) were collected in 2017 (Fig. 1).

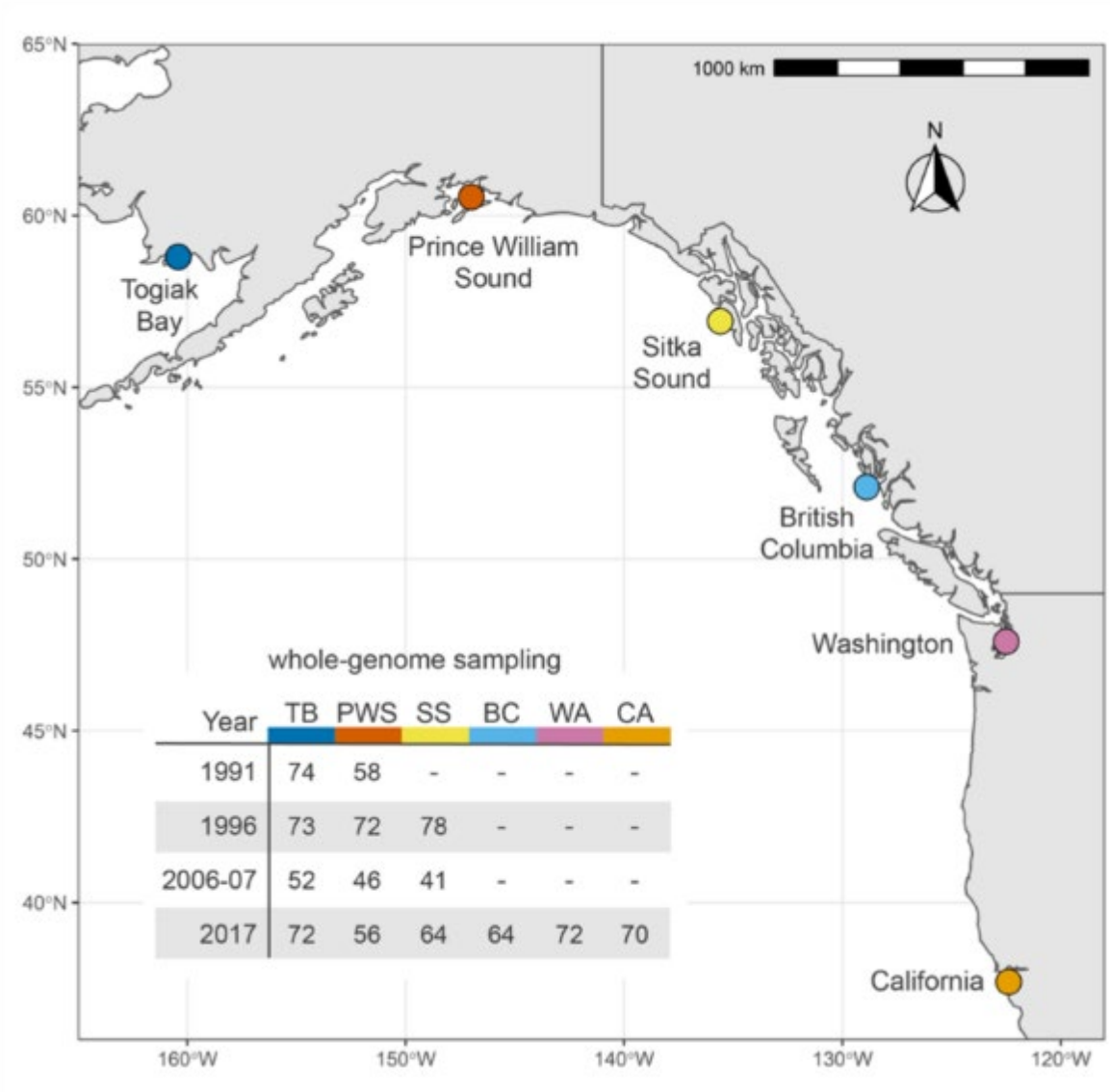

Figure 1. Map of Pacific herring sampling locations for population genetics, where inset table includes the number of individual samples sequenced per year per population.

Table 1. Pacific herring tissue sources used for population genetics. Samples were collected by the Alaska Department of Fish and Game (ADF&G), U. S. Geological Survey (USGS), Fisheries and Oceans Canada (DFO), National Oceanic and Atmospheric Administration (NOAA), and California Department of Fish and Wildlife (CADFW).

Region	Year	Location	Latitude	Longitude	Tissue	Collector	Date
Togiak Bay, AK, USA	1991	Togiak Bay	59.035	-160.393	Muscle	ADFG	06/91
Togiak Bay, AK, USA	1996	Togiak Bay	59.035	-160.393	Muscle	ADFG	05/96
Togiak Bay, AK, USA	2006	Nunavachak	58.85	-160.05	Fin	ADFG	05/06
Togiak Bay, AK, USA	2017	Togiak Bay	N/A	N/A	Muscle	ADFG	05/17
Prince William Sound, AK, USA	1991	Green Island	60.265	-147.4231	Muscle	ADFG	10/91
Prince William Sound, AK, USA	1996	Rocky Bay	60.3469	-147.1028	Muscle	ADFG	04/96
Prince William Sound, AK, USA	2007	Gravina Point	60.64	-146.272	Fin	ADFG	03/07
Prince William Sound, AK, USA	2017	Gravina Point	60.64	-146.272	Fin	USGS	04/17
Sitka Sound, AK, USA	1996	Sitka Sound	57.0532	-135.3354	Muscle	ADFG	03/96
Sitka Sound, AK, USA	2006	Sitka Sound (North Crow Pass)	57.12	-135.47	Fin	ADFG	03/06
Sitka Sound, AK, USA	2017	Sitka Sound	57.0532	-135.3354	Fin	USGS	03/17
Kitasu Bay, BC, Canada	2017	Kitasu Bay (Jamieson Point)	52.56	-128.75	Muscle	DFO	03/17
Puget Sound, WA, USA	2017	Puget Sound (Holmes Harbor)	48.07	-122.53	Fin	NOAA	04/17
San Francisco Bay, CA, USA	2017	San Francisco Bay	37.94	-122.48	Larvae	CADFW	06/17

Library preparation, sequencing, and alignment

DNA extraction and individually-indexed libraries were prepared using the methods reported elsewhere (Therkildsen and Palumbi 2017), and libraries were sequenced using Illumina HiSeq 4000 (PE-150 reads). Whole genome sequencing of 892 individuals resulted in 9,065,600,620 raw reads that were trimmed using Cutadapt (v. 1.8.3, Martin 2011). Trimmed reads were mapped to the Atlantic herring reference genome (*Clupea harengus* chromosome level genome assembly Ch_v2.0.2, Pettersson et al. 2019); chromosomes = 26; total base pairs = 725,670,187; protein coding genes = 24,095; gene transcripts = 67,663) using the Burrows-Wheeler Alignment Tool (v. 0.7.17, Li and Durbin 2009). We marked duplicates with Picard Tools MarkDuplicates (v. 2.7.1, broadinstitute.github.io/picard/), sorted alignments using Samtools (v.1.9, Li and Durbin 2009), and assessed the quality of alignments with multiQC (Ewels et al. 2016) and Picard Tools CollectWgsMetrics. Mean per-individual sequencing coverage was 1.06× across all samples.

SNP calling and genotype likelihood estimation

After mapping the reads to the reference genome, we used the Genotype Analysis Toolkit (GATK) to call single nucleotide polymorphisms (SNPs) and output phred-scaled genotype likelihoods (v. 4.1.4.1, Poplin et al. 2018). We generated genomic variant call files (VCFs) from sorted alignments using Haplotype Caller and followed the GATK4 Best Practice Workflow for variant calling which uses GenomicsDBImport to merge GVCFs from multiple samples. We used GenomicsDBImport to create a database for each of the 26 chromosomes and genotype VCFs to call raw variants across all samples for each chromosome. Raw variants were filtered to include biallelic SNPs at sites with Phred-scaled quality > 20, mapping quality > 30, depth > 600, and depth < 7000. These filtered variants were concatenated into one VCF containing all chromosomes with 'bcftools concat' (v. 1.10.2, Li 2011). We subset this VCF into two separate ways: 1) 14 VCFs containing samples grouped by population location and year collected and 11 VCFs containing time series samples from three Alaska populations. We filtered each VCF to include sites with genotyping rate > 50%, and intersected the 14 or 11 filtered VCFs with 'bcftools isec' to keep sites common across all populations. Finally, we filtered out sites with a minor allele frequency < 0.05. Our final VCF files included 330,482 and 394,005 biallelic SNPs. All scripts used to generate the final VCF from raw fastq files are available at https://github.com/joemcgirr/pac_herring and https://github.com/kahot/PacHerring.

Population structure and genome-wide summary statistics

We converted genotype likelihoods from the final VCF into BEAGLE format and used PCAngsd (Meisner and Albrechtsen 2018) and NGSadmix (Skotte et al. 2013) to analyze population structure. We evaluated the optimal cluster number (K) using evalAdmix (Garcia-Erill and Albrechtsen 2020) and CLUMPAK (Kopelman et al. 2015). We used Analysis of Next Generation Sequencing Data software (ANGSD v. 0.931, Korneliussen et al. 2014) to calculate Tajima's D, relative genetic divergence (Fst), and the population branch statistic (PBS). We subsetted the final VCF into 14 populations (grouped by location and year collected) and used

ANGSD to calculate a folded site frequency spectrum and per site allele frequencies from genotype likelihoods. We used these frequencies to estimate Tajima's D in 50kb sliding windows with a 10kb step size. We created two-dimensional site frequency spectra for each population pair and calculated Fst and PBS in 50kb sliding windows with a 10kb step size. We calculated absolute genetic divergence (Dxy) from allele frequencies output by ANGSD using the CalcDxy.R script in ngsTools (Fumagalli et al. 2014). Within-population nucleotide diversity (π) was estimated using Pixy (Korunes and Samuk 2021).

Allele frequency shifts and linkage disequilibrium

We used 'bcftools query' to output allele frequencies for the 14 populations and calculated Δz, the arcsine transformed allele frequency difference between sampling periods arcsine(sqrt(t1 – t0)). We averaged Δz in 50kb sliding windows with a 10kb step size. We used PLINK (v.1.9, Purcell et al. 2007, Chang et al. 2015) to estimate linkage disequilibrium (LD) for the 14 populations. We used '--indep-pairwise 100 10 0.8' to calculate r2 (squared allele count correlations).

Identification of structural variants

Large structural variants (potential inversions) were identified by visualizing the SNP patterns over a chromosome using vcfR and PopGenome packages in R.

Selection scan

Genome-wide selection scans were conducted using PCAngsd. Fst outliers were also assessed by creating a null model for the maximum change in a region expected across the genome (Pinsky et al. 2021). Briefly, the pairs of unlinked SNP allele frequencies were shuffled across the unlinked SNP locations in the genome, and the maximum Fst over a specified window across the entire shuffled genome were recorded for 1000 times and this empirical distribution of maximum Fst was used to assess significantly high Fst values.

Genome-wide linked selection using temporal covariances of allele frequency changes

We assessed the genome-wide covariance of allele frequency changes from the timeseries data to determine whether signals of linked selection could be detected. The temporal covariances were calculated using the CVTKPY pipeline (Buffalo and Coop 2019, 2020) for each population using 100kb tiles. In addition to the genome-wide averages, we calculated the average covariances based on 100kb windows, which were used to identify the outlier regions that fell within the top 1% of the total covariances for each population within each time period. Genes in the outlier regions were identified using SnpEff v. 5.1 (Cingolani et al. 2012) and Gene Ontology enrichment analysis was carried out using ShinyGo v.0.76.3 (Ge et al. 2020).

Aims 2 and 3

Animal Collection and Care

Pacific herring were collected near Krestof Island in SS, Cedar Bay in PWS, and Cherry Point in Puget Sound, Washington (WA). Collection of ripe herring by gill net occurred on April 9th for

SS, April 12th for PWS, and May 9th for WA in 2018. Ovaries and testes were dissected and stored in humidified whirl packs or petri dishes prior to transport for the Alaska fish and within an hour after transport for WA fish (number of females used: 16 for SS, 11 fop PWS, and 10 for WA). Average ovary masses were 30.5 ± 1.2, 37.0 ± 1.6, 34.5 ± 1.7 grams for SS, PWS, and WA, respectively. Prior to fertilization, a subsample of eggs was counted and weighed to determine average egg mass which was 0.0012, 0.0017, and 0.0009 g for SS, PWS, and WA, respectively. Egg mass was used to calculate total mass of fertilized eggs used for each population which was 113.4, 183.8, and 108.45 g for SS, PWS, and WA, respectively. Since egg size varied between sites, this allowed us to maximize our embryo output and normalize density between sites.

Fertilizations were performed in water tables at Marrowstone Field Station (U. S. Geological Survey Western Fisheries Research Center, Nordland, Washington) as described elsewhere (Griffin et al. 1998). Polyvinyl alcohol with $Ca2^{+}$ and Mg^{2+} -free seawater was used to prevent clumping of eggs which were evenly distributed onto 24 sheets of 1 mm nylon mesh, each of which could hold 10-20 g of embryos. At least 5 males were used for fertilization and gametes were evenly distributed amongst the egg-covered sheets. Fertilized eggs were left undisturbed for 1 hour and then transferred to 1.2 m diameter tanks with filtered seawater overnight for 8-12 hours. Fertilization rates were then assessed microscopically and oil exposure was conducted on batches with rates above 75% (SS: 85%, PWS: 85%, WA: 96%). Embryonic crude oil exposures spanned between 1 day post fertilization (dpf) and 10 dpf in filtered seawater at ambient temperatures, which were 9.2 ± 0.2, 9.3 ± 0.2, and 10.8 ± 0.3°C during the SS, PWS, and WA exposures, respectively. Temperature was recorded twice per hour in a downstream tank from the exposure system by a Hobo Water Temp Pro v2 sensor (Onset). Animal care and use protocols were approved by the Western Fisheries Research Center Institutional Animal Care and Use Committee (protocol# 2008-51).

Oil Exposure

Prior to exposures, Alaskan North Slope crude oil (ANSCO) was weathered, as is standard practice, by heating to 60°C in a water bath until the volume decreased by 10%. The exposure system (SINTEF, Trondheim, Norway) produced a continuous, flow-through of dispersed oil droplets (Nordtug et al. 2011). It consisted of 24 10 L tanks with individual flow of filtered seawater (360 µL/min flow rate) at ambient temperature, and ANSCO effluent flow at 60 µL/hr injection rate. ANSCO effluent entered the system through a dispersion generator which produced microdroplets of oil which were pumped into a 2 L reservoir that was gravity-fed to a series of solenoid valves which controlled the ratios of effluent to filtered seawater into the exposure tanks. Six concentrations (n=4) were generated ranging from 0.01 (no oil) to 3.5 µg/L ∑PAHs (polycyclic aromatic hydrocarbons). Fertilized eggs adhered to nitrex sheets were distributed among the tanks (1 sheet per tank) and monitored several times daily from the beginning of oil exposure at 1 dpf until 10 dpf at which time oil injection stopped. Exposure dates for each population were 4/10/18 to 4/20/18 for SS, 4/13/18 to 4/23/18 for PWS, and

5/11/18 to 5/21/18 for WA populations. During the overlapping exposure days for SS and PWS (4/13/18 – 4/20/18), there were two nitrex sheets with adhered eggs per tank.

Analysis of PAHs

Water samples were collected in the mid-water column by siphoning 100 mL into 125 mL amber bottles with 20 mL of dichloromethane for stabilization (high-performance liquid chromatography-grade, Burdick & Jackson, Muskegon, MI). Samples were analyzed for 58 PAH analytes (Sloan et al. 2014). Briefly, samples were extracted with methylene chloride using an accelerated solvent extractor for tissue or separatory funnels for water samples. Highly polar compounds and lipids were removed from PAH extracts with silica/aluminum columns and size-exclusion high-performance liquid chromatography, respectively. PAH separations were conducted on a 60 m DB-5 chromatography (GC) capillary column before detection on an electron impact mass spectrometer (MS) in selected-ion monitoring mode. Concentrations below the detection limit were reported as <LOQ (less than the limit of quantification). ∑PAH values were calculated from >LOQ values only. For body burdens of ∑PAHs, 100 embryos at 10 dpf (n=4) were collected from each nitrex sheet and stored in 2 mL cryotubes at -80°C. Samples were analyzed for 49 PAH analytes using liquid extraction prior to normal phase solid phase extraction (LE-SPE) (Sørensen et al. 2016). For all three populations we measured ∑PAHs in fish bodies and in water at 10 dpf from all five oil levels and controls (Fig. 2A). Additionally, we measured ∑PAH body burdens in AK-PWS fish at four more timepoints during developmental exposures (1, 1.5, 2, 3, and 4 dpf) from the high dose (Fig. 2B).

Characterization of Cardiovascular Developmental Perturbation

At 10 dpf and at hatch (12-14 dpf), 20 embryos/larvae from each tank (n=4) were immobilized with 0.01% tricaine mesylate (MS-222) and mounted laterally in petri dishes with methyl cellulose or 1.5% agarose gels with slots molded by glass capillary tubes. Seawater was maintained between 9-11.5°C depending on current ambient temperature of source tanks by a microscope stage chiller. For each larva, 10 second videos focusing on the atrium and ventricle were taken with Unibrain Fire-i400 1394 cameras (San Ramon, California) at the highest magnification (6-8x) on Nikon SMZ-800 stereomicroscopes (Irvine, California). BTV Pro software (Bensoftware.com) was used for imaging. Lateral images were also taken for whole body and craniofacial morphology at 1-2x and 5x magnification, respectively. Treatments were imaged randomly throughout an 8-hour period.

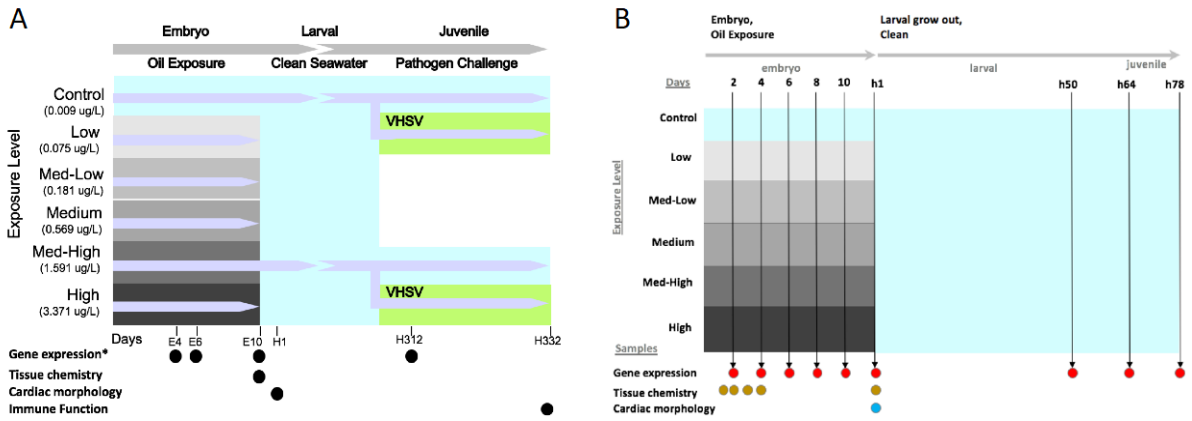

Figure 2. Experimental designs for oil and virus exposure experiments. A: All three populations (Prince William Sound [PWS], Sitka Sound, and Washington state) were exposed during embryogenesis to no-oil clean controls conditions and five oil concentrations. Exposures started 1 day post-fertilization (dpf) through to 10 dpf, then fish were transferred to clean seawater. Fish were sampled for gene expression at 4, 6, and 10 dpf, tissue chemistry was measured at 10 dpf, and cardiac endpoints were measured on the first day post-hatch (H1). Fish from the control condition and the medium-high oil dose were raised in clean conditions through to juvenile stage and exposed to viral hemorrhagic septicemia virus (VHSV). B: Additional samples were collected for PWS fish. Gene expression was sampled at 2, 4, 6, 8, and 10 dpf from all exposure treatments, including three timepoints post-hatch. After 10 dpf fish were raised in clean water. Tissue chemistry was also sampled at multiple timepoints during embryogenesis, including 1, 1.5, 2, 3, 4, and 10 dpf.

Heart videos were blinded for treatment and randomly analyzed for function and morphology using ImageJ software (National Institutes of Health?). Prior to measurements, video was assessed for appropriate quality and contrast and excluded if the morphology of interest was not visible. Endpoints measured at 10 dpf included heart rate, pericardial area, and atrial and ventricular fractional shortening for SS and WA embryos. An overlap in sampling days prevented adequate data collection for PWS fish at this time point. For larvae at hatch, atrium and ventricle areas during systole and diastole, posterior ventricle outgrowth, and fractional shortening were measured. Heart rate was measured by counting the number of frames over the course of ten cardiac cycles once for each embryo or larva. Pericardial area, an indicator of edema, was measured by drawing a perimeter around the pericardium with the yolk as the posterior end. Atrial and ventricle chamber areas were measured by drawing around the perimeter during systole and diastole three times for each embryo and larva. Fractional shortening, the % difference in diameter between diastole and systole, was calculated for both the atrium and ventricle. Posterior ventricle outgrowth was measured by drawing a perimeter within the ventricle at diastole starting at the posterior side of the atrioventricular (AV) valve to the apex of the ventricle to assess ballooning of the ventricle beyond the AV valve.

Virus Challenge

Herring used in this study were from 3 different putative populations: PWS, SS, and WA. For these experiments, herring from each population were the survivors of embryonic exposure to oil from the SINTEF generator at each of two concentrations: (no-oil controls - ∑PAH 0.02 µg/g, and medium-high oil - ∑PAH 1.9 µg/g). Virus exposures were in triplicate tanks per treatment (population by oil exposure history), with each tank containing 70 herring. Three mL of stock VHSV (batch 2019BB, titer 2.4x108 PFU / mL) were added to the treatment tanks to achieve 2.66x 103 PFU/mL (Hershberger et al. 2013). No virus was added to control treatments. Daily mortalities were recorded, and VHSV tissue titers (kidney / spleen) were collected for each of these fish. Immunocompetent tissues (kidney) were harvested throughout the experiment for gene expression analysis. Mortalities were arc sin transformed for each treatment including controls and plotted as cumulative mortalities.

RNA Sequencing

Pacific herring samples were stored at -80°C prior to homogenization using 1.4 mm ceramic beads (Genaxxon Bioscience) on a TissueLyser (Qiagen). Ground lysates were suspended in 200 µl of lysis binding buffer, incubated at room temperature for 10 minutes, centrifuged for 10 minutes at 13,000 rpm, and the supernatant was retained. mRNA was extracted separately from each sample using oligo (dT) 25 beads (DYNABEADS direct™) to enrich for polyadenylated mRNA.

Strand specific RNA-seq libraries were prepared using the BRaD-seq protocol (Townsley et al. 2015), and used 14 cycles of PCR at the enrichment phase. Library preparations for all populations were identical. A random hexamer was used to prime fragments from along the length of the transcript:

GTGACTGGAGTTCAGACGTGTGCTCTTCCGATCTNNNNNNNN, where N represents a random nucleotide (Townsley et al. 2015). Finished libraries were quantified using the Quant-iTTM PicoGreen dsDNA high sensitivity kit (ThermoFisher) and normalized to 1ng/µl. We used 2ng per library and multiplexed up to 96 samples for sequencing. Each multiplexed group of samples included replicate samples from each treatment. The libraries were sequenced in 4 lanes of an Illumina HiSeq X platform (Illumina, Inc.), generating 10.8 million paired reads per sample. Raw reads were quality checked with FastQC v.0.11.5 (Wingett and Andrews 2018). Low quality reads (q<20), adapters, and reads less than 25-bp were removed using Trimmomatic v.0.36 (Bolger et al. 2014).

We created a high-quality annotated reference transcriptome for Pacific herring using Pacific Biosciences Iso-Seq technology to provide a mapping reference for transcriptomics experiments. Whole embryo RNA was isolated from a single embryo with the RNeasy Plus Micro Kit (Qiagen), quantified by fluorometry with a Qubit (RNA Broad Range Assay Kit, Molecular Probes) and quality assessed with a 2100 Agilent Bioanalyser (RNA Nanochip, Agilent Technologies). First-strand cDNA synthesis was performed with the TeloPrime Full-Length

cDNA Amplification Kit (Lexogen) using the cap-dependent linker ligation method. cDNAs were quantified for each sample and equimolar concentrations were combined into a single pool prior to library preparation. Single Molecule Real Time (SMRT) bell libraries were prepared by U. C. Davis DNA Technologies Core with the SMRTbell Express Template Prep Kit 2.0 (Pacific Biosciences). Sequencing was completed on the Sequel II System on a single SMRT Cell 8M. Polished circular consensus reads were demultiplexed, refined, and clustered into high quality reads representing isoform-specific transcripts using the Pacific Biosciences IsoSeq v3.1.1 default parameters. For *de novo* transcript annotation, we employed the dammit pipeline (https://dib-lab.github.io/dammit/). Briefly, gene models were built with Transdecoder (https://github.com/TransDecoder/TransDecoder), which were annotated based on evidence from four protein databases (Pfam-A, Rfam, OrthoDB, Uniref90) and the reference genome from Altantic herring (*Clupea harengus*), accession number GCA 900700415.1 version Ch v2.0.2. We then used the Benchmarking Universal Single-Copy Orthologs (BUSCO v3) software to compare the gene content in our *de novo* transcriptome with a lineage-specific data set (Actinopterygii) (Simão et al. 2015). The complete isoform-aware assembled transcriptome consists of a total of 180,175 transcripts, a contig N50 of 3,663, BUSCO completeness score of 95%, and 75% of the transcripts annotated with gene IDs.

For RNA-seq transcriptomics, trimmed sequence reads were mapped to the reference transcriptome and mapped reads quantified with Salmon (Patro et al. 2017) using the reference transcriptome and default settings. The length-scaled TPM function in tximport was used to sum the transcript counts to the gene level (Soneson et al. 2015). Only genes with sufficient counts (> 100k) were retained for further statistical analysis using the filterByExpr function in edgeR (Robinson and Oshlack 2010). The gene count data were normalized using the weighted trimmed mean of M-values (TMM) and converted to log2-counts per million (log2CPM) using the limma R package (Law et al. 2014, Ritchie et al. 2015).

Data analysis and statistics

Water and tissue PAH composition was assessed in R (Version 3.5.2) using the 'vegan' package for non-metric multidimensional scaling (nMDS). Blank corrections were conducted for tissue PAHs when the blank value was higher than the detection limit (included: naphthalene, methylnaphthalenes, C3-BT, C2-PHE, and C2-PYR). Available PAH concentrations for water and tissue were screened for near-zero and near-LOQ values. PAHs were excluded from data when high dose treatments (1.5 and 3.5 µg/L ∑PAHs) had >75% of detections below the LOQ. Included PAHs (48 for tissue, 61 for water) were square root transformed prior to analysis. Scree plots were used to optimize the level of stress and number of dimensions. In all cases, 3 dimensions were used with corresponding stress values ranging from 0.02 – 0.04. Differences between population, treatment, and population by treatment interaction were evaluated using PERMANOVA. All nMDS plots were generated using the 'ggplot2' package.

For RNA-seq data, we analyzed two sets of samples. In our first set, which focused on dense sampling across time, we analyzed PWS fish only at five time points during embryogenesis (2, 4,

6, 8, and 10 dpf) and at four time points post-hatch (1, 50, 64, and 78 dph) (Fig. 2B). We sampled fish from the five oil doses and a no-oil control. For these samples we also measured body burdens of ∑PAH at 5 points during embryogenesis (1, 1.5, 2, 3, 4, and 10 dpf). For the second set of samples, which focused on population contrasts, we sampled fish from all three populations (PWS, SS, and WA) from three times during embryogenesis (4, 6, and 10 dpf) and from all five oil doses and the no-oil control (except for at 4 dpf where we sampled only two doses plus the no-oil control) (Fig. 2A). For each treatment we sampled eight fish, where two fish were sampled from each of four replicate tanks. We used multidimensional scaling to evaluate trends in the normalized counts by sample data and determined that the library preparation 96-well plate was a detectable source of variance. Therefore, a linear model was used to evaluate the effect of age (dpf), population, and oil treatment on gene expression, with plate as a random effect in the model. All p-values were corrected with the false discovery rate (FDR) algorithm. We then selected gene sets with significant treatment effects ($p<0.05$) and removed the plate effect from visual representations using the removeBatchEffect function (Limma; Ritchie et al. 2015). Further visualizations used the pheatmap package (Kolde 2012) in R to generate heat maps and the factoextra package (https://rpkgs.datanovia.com/factoextra/index.html) to generate PCA plots.

Linear regressions were performed to compare heart chamber areas, fractional shortening, and posterior ventricle outgrowth at hatch with increasing tissue concentration of ∑PAHs between populations using Prism 8 (GraphPad). A two-way analysis of variance (ANOVA) using R Studio (base package; version 1.4.1717) was used to determine the effect of oil, source population, and their interaction, with tank treated as a random effect for parameters at 10 dpf. When oil effects were present, a Tukey's post hoc test ($p<0.05$) was used to compare means between treatments.

RESULTS

Aim 1

We collected whole genome sequences from 892 samples from 14 population groups (sorted by location and year) using low-coverage whole genome sequencing, resulting in per-individual average depth coverage of 1.061x. After read mapping, sites were filtered to genotyping level of 0.5 for each population and year combination. After filtering steps, a total of 330,482 loci were included in the subsequent analyses.

Overall population structure and nucleotide diversity

Strong population structure was detected (Fig. 3A) between TB and the rest of the herring populations (Pairwise Fst: 0.125-0.198), suggesting limited gene flow across the Alaska Peninsula. Of the remaining populations between the Gulf of Alaska and California, the California population was most distinct from the rest (Pairwise Fst: 0.030-0.0325), while small differentiation was detected between the Gulf of Alaska and Washington (Pairwise Fst: 0.0088-

0.011). This population structure was also supported by the results from NGSadmix, which estimates individual admixture proportions. The results from NGSadmix and subsequent evaluation by Clumpak showed that three primary ancestral clusters, with minimal gene flow from the TB population to others (Fig. 3B).

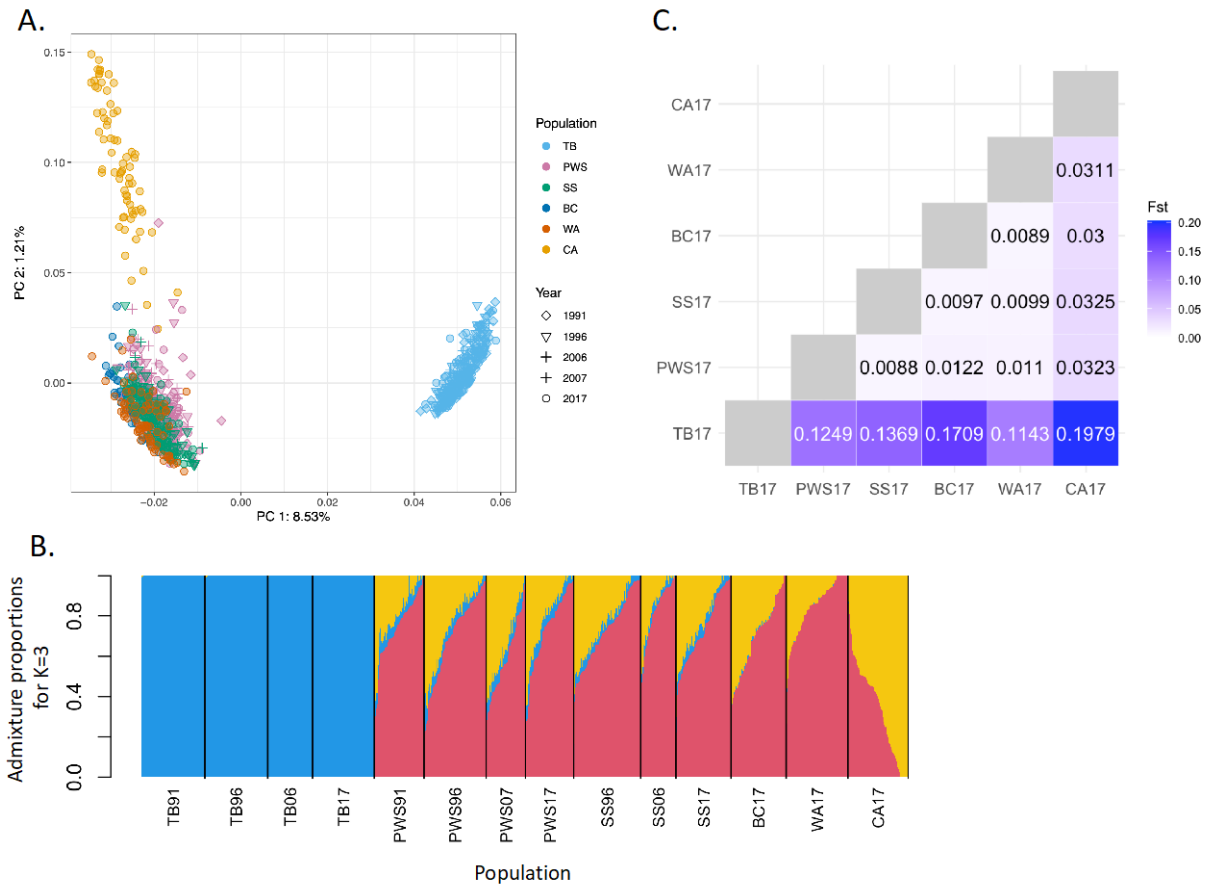

Figure 3. Population genetic structure from whole-genome sequence data. A: results from principal components analysis, where populations are indicated by colors, and year of sample collection by symbols. B: results from NGSadmix analysis, where K=3. C: Fst between pairs of populations (2017 collections). Higher FST values implies a higher degree of differentiation among populations.

The levels of nucleotide diversity were similar across all populations, ranging from 0.00324 to 0.00369 (estimated by Pixy), where no substantial differences in π was detected between time periods within the three Alaska populations. The site frequency spectrum (1D SFS) of each population at each time point revealed TB populations to have less rare alleles, compared to the others, suggesting a recent reduction in population size. SFS in the PWS population showed a slight loss of rare alleles from 2007 to 2017, consistent with reduction in population size.

Genetic change through time – population structure

PCA (PCAngsd) and model-based admixture (NGSadmix) analysis in ANGSD showed no substantial changes in genetic structure over time within a population. Genome-wide pairwise Fst values showed little change over time within each population (Fst: 0.0066-0.0117). However, the Fst values within PWS population (0.0081-0.0117) were higher than SS (0.0066-0.0103) and TB (0.0067-0.0104) populations, indicating relatively greater genetic variance in the PWS population over this time period.

Genetic change through time – effective population size

The effective population size (Ne) estimated from allele frequency changes (Jorde and Ryman 2007) showed little change in TB and SS populations, while Ne of the PWS population showed an increase and then a decline over time (Fig. 4). Although the relative differences in Ne between populations and time points are likely to be accurate, the absolute numbers for Ne estimated using this method are unlikely to be accurate due to the small sample size relative to census population size (Marandel et al. 2019).

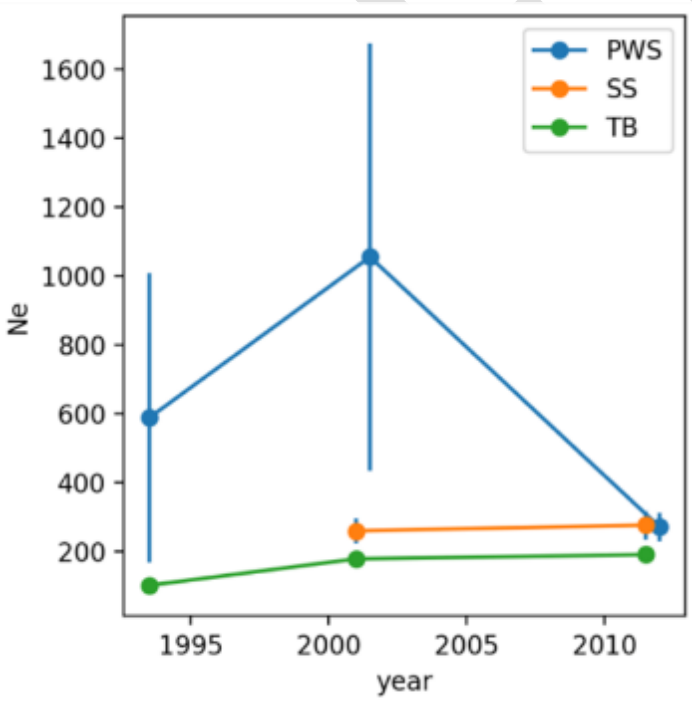

Figure 4. Effective population size (Ne) for Alaska populations in Prince William Sound (PWS), Sitka Sound (SS), and Togiak Bay (TB) estimated from allele frequency change between successive time periods.

Genetic change through time

Temporal covariance revealed signatures of natural selection whereas more traditional PC-based selection scans did not. No significantly selected loci were identified from PC-based genome-

wide selection scans between years within any of the three (PWS, SS, TB) populations. Temporal covariances revealed that the PWS population showed a signal of genome-wide positive selection (adaptive responses) over time, whereas other populations (TB and SS) did not (Fig. 5). Since the program that we used to detect linked selection using allele frequency covariances was established based on the assumption of non-overlapping generations, we assessed how overlapping generations might have impacted the observed patterns of temporal covariances using simulations in SLiM. Both overlapping and non-overlapping generation models produced highly similar covariance patterns, consistent with valid application of this analysis for Pacific herring.

We assessed the identity of genes located in the outlier regions of highest covariances (top 1%) identified in each time period (Fig. 6) and conducted Gene Ontology (GO) enrichment analysis with ShinyGo (Ge et al. 2020). The genes in the outlier regions identified from the first time period (1991-1996 vs. 1996-2006) in PWS population were significantly enriched for the Molecular Function terms *C-C chemokine receptor activity*, and *Alpha-sialidase activity*. No significantly enriched GO terms were identified from the genes in the outlier regions identified from the second time period (1996-2006 vs. 2006-2017) below the cutoff value (FDR <0.05), but the Biological Process term *Anatomical structure morphogenesis* was implicated (FDR = 0.069). No GO terms were enriched in the top 1% of covariance regions for TB and SS populations for any time period.

Structural variation among populations

We detected evidence of a large inversion chromosome 12 segregating within and between populations. The inversion was observed primarily in the California population (Fig. 7A). Over 90% of California individuals harbored at least one copy of this inversion. This inversion was detected in heterozygous form in individuals from all other populations and time points, but in less than 25% of individuals. Another large chromosomal inversion was detected on chromosome 7 (Fig. 7B), and similar to the chromosome 12 inversion it was primarily found in individuals from the CA population. Over 90% of individuals in CA harbored at least one copy of this inversion. Approximately 30-40% of TB individuals harbored at least one copy of this inversion, which is a higher frequency than for all other populations except CA.

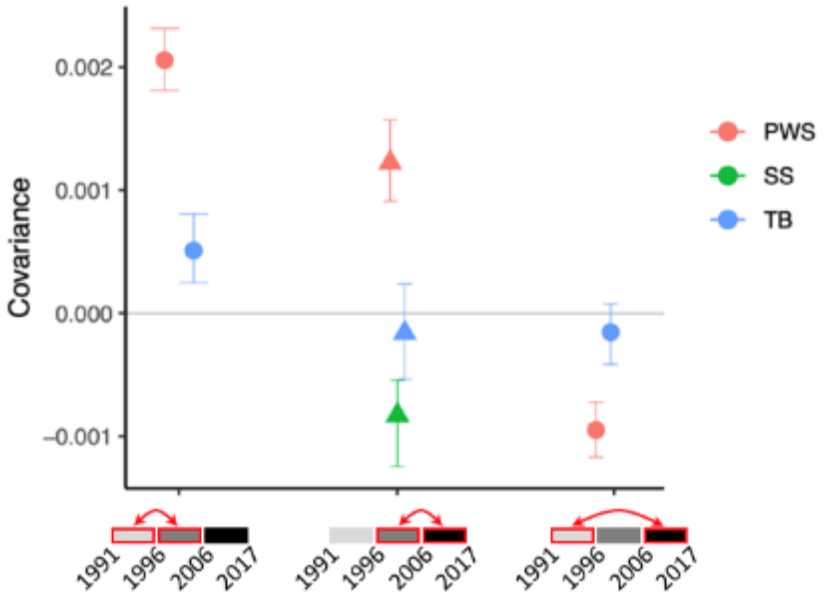

Figure 5. Positive temporal covariances, indicating the influence of polygenic selection, were detected for the Prince William Sound (PWS) population across the first three time periods and the second three time periods. Negative covariance for the PWS population over the whole time period (1991/1996 to 2006/2017) indicated switching selective regimes over time. Slightly positive (Togiak Bay [TB] 1991/1996 to 1996/2006), zero, or negative temporal covariances were detected for all other populations (e.g., Sitka Sound [SS]), indicating limited signal of polygenic selection, or signal of selection that could not be distinguished from genetic drift.

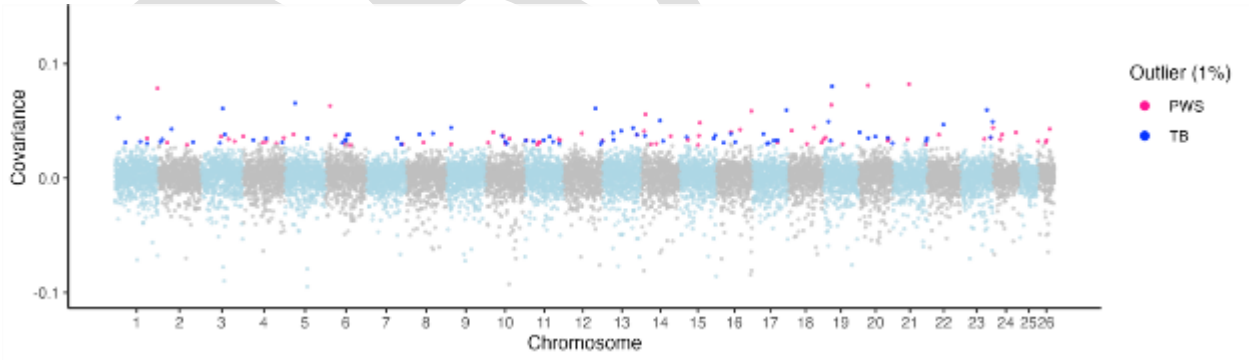

Figure 6. Genome-wide visualization of the top 1% of temporal covariance outlier regions (regions of the genome showing the strongest signals of polygenic adaptation) for the first period (1991-1996 vs. 1996-2006). Outlier regions for Prince William Sound (PWS), and Togiak Bay (TB) populations are highlighted in red and blue, respectively.

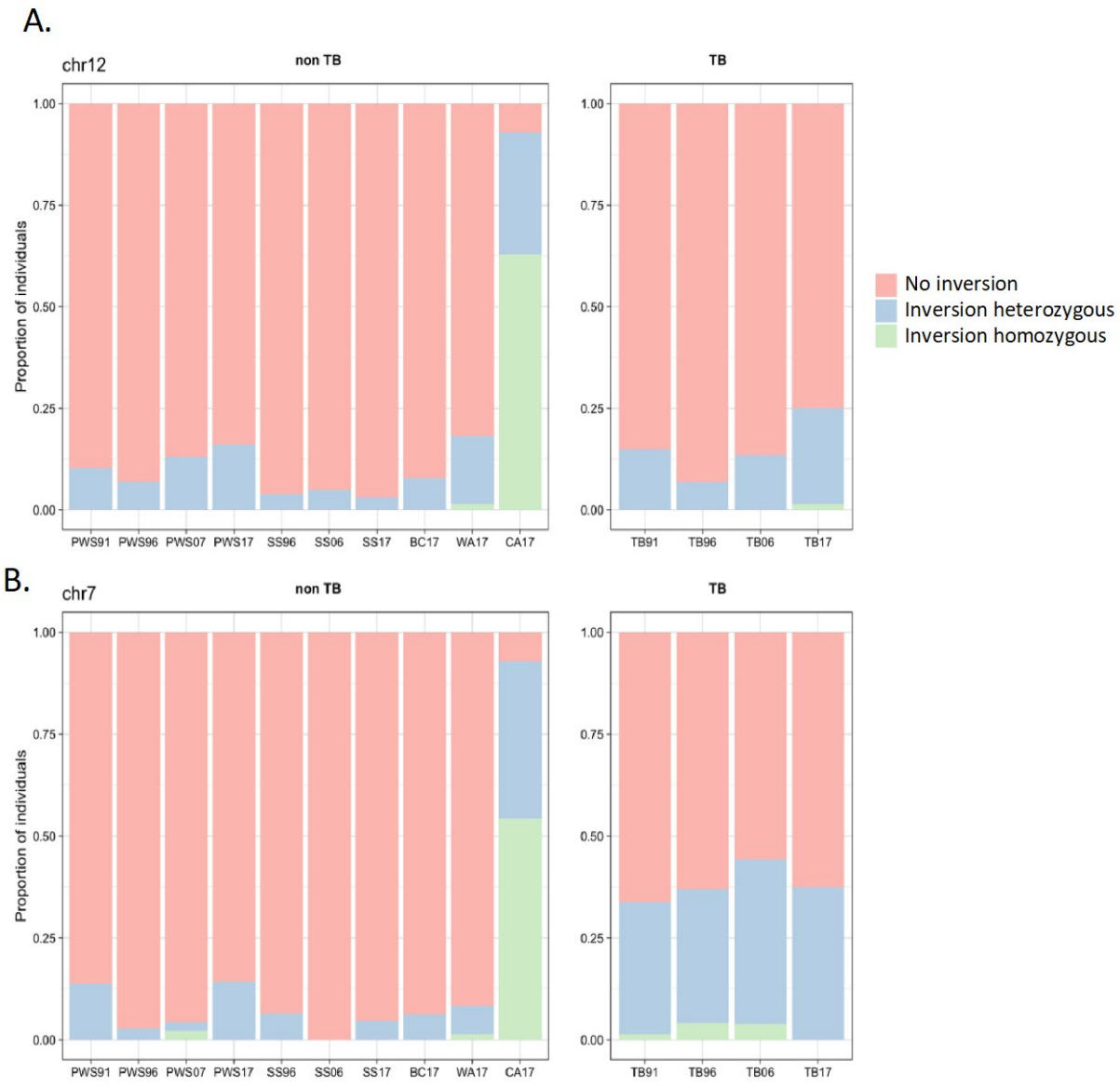

Figure 7. Frequency of putative chromosomal inversions on chromosome 12 (A) and chromosome 7 (B). The frequency of individuals that have zero, one, or two copies of the inversion are indicated in orange, blue and green, respectively.

Aims 2 and 3

Oil concentrations and doses

For exposures for PWS and SS populations, the water concentrations for oil treatments ranged from 0.06 ± 0.004 µg/L ∑PAH in the lowest concentration treatment to 3.42 ± 0.05 µg/L in the highest concentration treatment (Table 2, Fig. 8). For the WA population exposures, the water

concentrations of oil ranged from 0.07 ± 0.004 µg/L ∑PAH in the lowest concentration treatment to 3.50 ± 0.05 µg/L in the highest concentration treatment. All three populations were therefore exposed to nearly identical oil concentrations. Accumulated dose in embryo tissues was measured at 10 dpf for all three populations (Figs. 8, 9A). Though water concentrations were nearly uniform for all three populations (Figs. 8A, 8D), accumulated body burdens differed between populations. PWS and SS fish had similar body burdens of PAHs by 10 dpf (Figs. 8B, 8C, 9A), but the WA population fish had lower overall ∑PAH concentrations in their tissues, and a shift in the profile of PAHs compared to the Alaska populations (Figs. 8E, 9A). This suggests that metabolism and elimination of PAHs may be greater in WA fish compared to Alaska fish. Indeed, metabolism of PAHs during embryogenesis is apparent; the temporal profile of PAH accumulation, which was characterized in only PWS fish, showed accumulation up to 4 dpf, followed by a substantial decrease between 4 and 10 dpf (Fig. 9B), despite exposure to constant PAH concentrations in the external waters over this exposure period.

Table 2. ∑PAH concentrations for water (µg/L) and embryo tissue (ng/g wet wt.) at 10 day post fertilization (dpf) for populations including Sitka Sound, Alaska (SS), Prince William Sound, Alaska (PWS), and Cherry Point, Washington (WA). Data presented as mean ± standard error of the mean.

	Water (1st expt)	Water (2nd expt)	Tissue SS	Tissue PWS	Tissue WA
	4/20/18	5/11/18	4/20/18	4/23/18	5/20/18
control	0.01 ± 0.0009	0.01 ± 0.0005	6.08 ± 0.9	2.7 ± 0.7	4.0 ± 1.4
low	0.06 ± 0.004	0.07 ± 0.003	15.7 ± 2.3	13.4 ±1.6	10.3 ± 2.3
medium-low	0.15 ± 0.006	0.18 ± 0.01	37.0 ± 8.4	27.5 ± 2.0	20.4 ± 2.4
medium	0.53 ± 0.02	0.72 ± 0.09	67.8 ± 25.4	64.5 ± 3.0	29.6 ± 2.7
medium-high	1.42 ± 0.09	1.67 ± 0.08	90.6 ± 6.2	105.0 ± 11.9	78.7 ± 30.4
high	3.42 ± 0.05	3.50 ± 0.3	180.8 ± 7.1	171.9 ± 15.0	153.1 ± 16.5

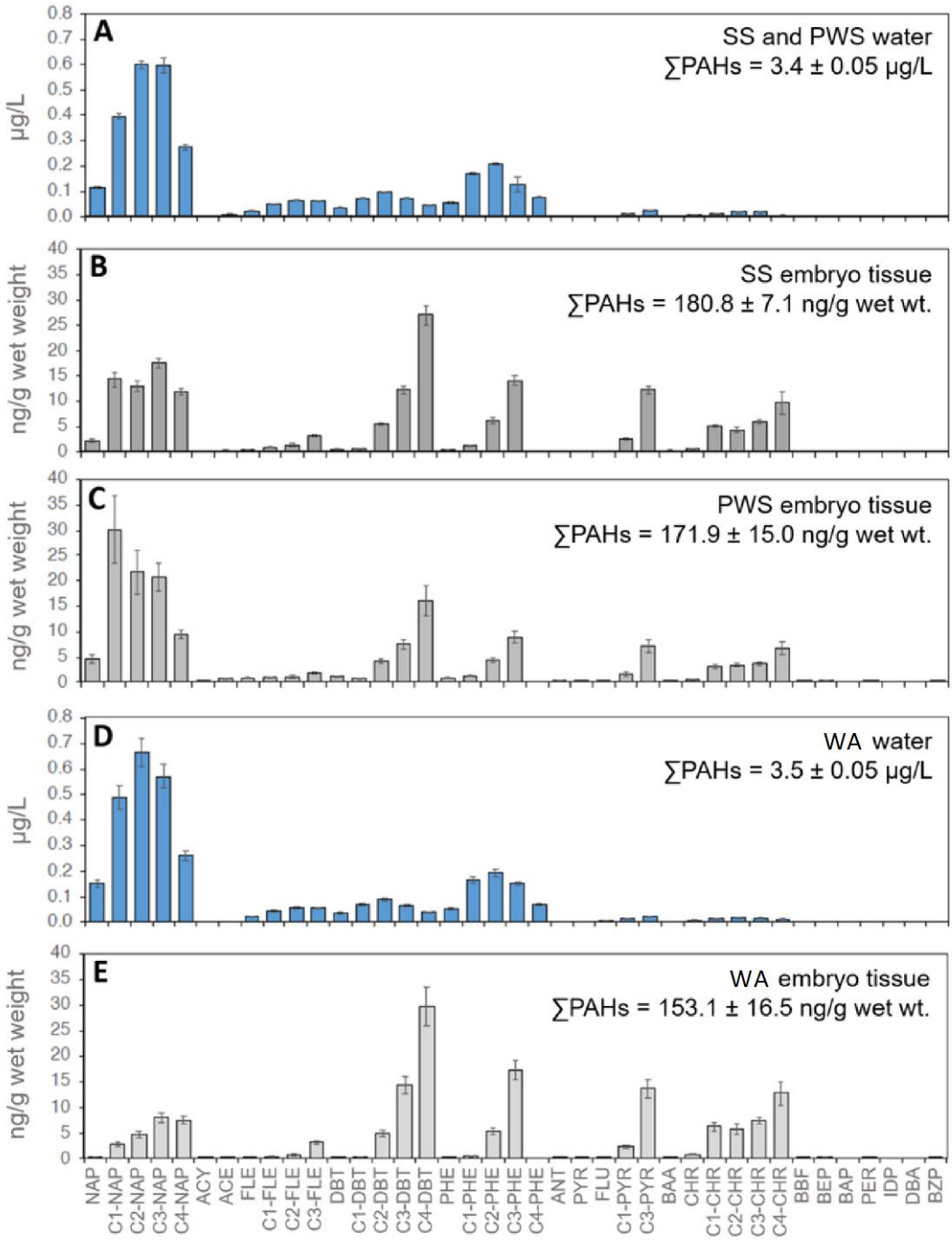

Figure 8. Water and tissue PAH concentrations for two exposure experiments. A-C: water and tissue concentrations for the first experiment that included both Alaska populations (PWS and SS). D-E: water and tissue concentrations for the second experiment that included the Washington (WA) population. A and D show water concentrations in µg/L for the two exposure experiments, and B, C, and D show tissue concentrations in embryos from the high dose at 10 dpf in ng/g wet weight for each of the three populations. Analytes included naphthalene (NAP), acenaphthylene (ACY), acenaphthene (ACE), fluorene (FLE),

dibenzothiophene (DBT), phenanthrene (PHE), anthracene (ANT), pyrene (PYR), fluoranthene (FLU), benz[a]anthracene (BAA), chrysene (CHR), benzo[b]fluoranthene (BBF), benzo[e]pyrene (BEP), benzo[a]pyrene (BAP), perylene (PER), indeno[1,2,3-cd]pyrene (IDP), dibenz[a,h]anthracene/dibenz[a,c]anthracene (DBA), benzo[ghi]perylene (BZP) in addition to their alkylated homologs indicated as C1-, C2-, etc.

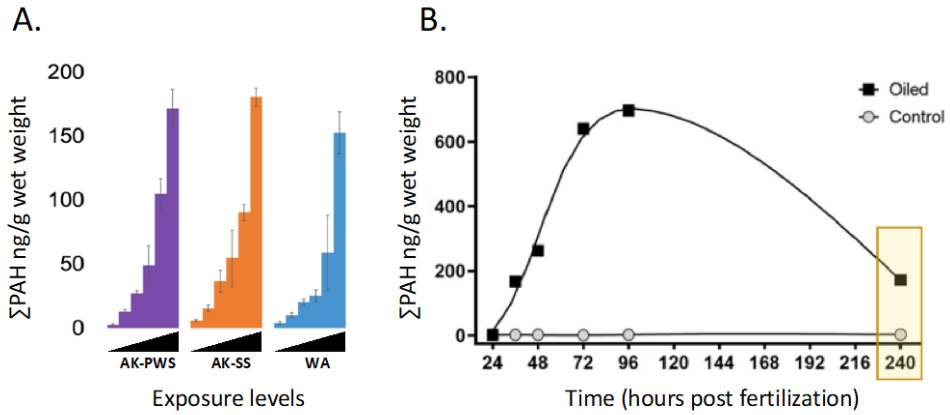

Figure 9. Variation in polycyclic aromatic hydrocarbon (PAH) body burdens among Prince William Sound (AK-PWS), Sitka Sound (AK-SS), and Washington (WA) populations and through development. A: Total PAHs among doses (wedges indicate increasing doses) for each population in embryos at 10 days post-fertilization (240 hours post fertilization). B: Total PAHs in PWS embryos through development, from 24, 36, 48, 72, 96, and 240 hours post fertilization, for embryos exposed to the high dose (black squares) and embryos exposed to no-oil controls (gray circles).

Oil exposure impacts on cardiovascular development

The earliest time point during development where circulation is detectable, indicating early stages of cardiovascular system development, is 4 dpf in Pacific herring. Pericardial edema, which is a sensitive indicator of crude oil impacts on the developing cardiovascular system, was not affected by oil exposures by 10 dpf ($p>0.05$), even in the highest dose. This indicates that our range of exposure concentrations was very low. Once fish are hatched and no longer coiled within the embryonic chorion, it is possible to orient individual fish such that different dimensions of heart morphology may be reliably measured. We characterized heart morphology at 1 day post hatch (dph). At our medium dose (64.5 ng/g, 0.53 µg/L) and higher, the area of the posterior ventricular outgrowth was significantly reduced ($p<0.05$) by oil exposure compared to controls in PWS and SS fish (Fig. 10). We found that the oil exposure impact on heart morphology varied between populations (significant dose-by-population interaction, $p<0.0001$), where the two Alaska populations (PWS and SS) were more sensitive than the WA population (Fig. 10A).

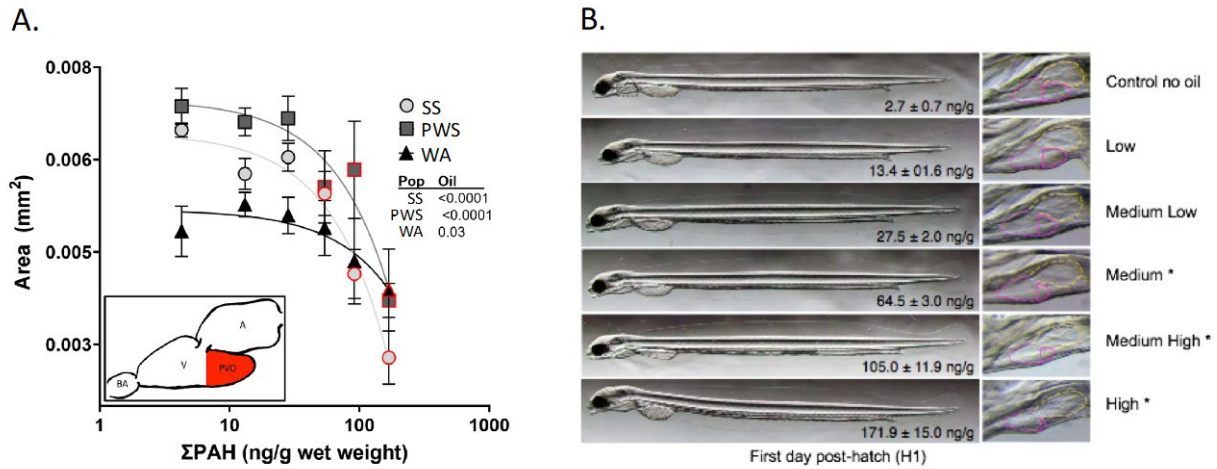

Figure 10. Perturbation of cardiovascular development in larval herring following embryonic exposure to crude oil. A: Area of the posterior ventricular outgrowth (PVO) decreased with increasing dose of crude oil (body burden of total PAHs measured as ng/g wet weight) in one day post hatch (dph) larvae. Inset figure is a drawing of the heart morphology (A: atrium, V: ventricle, SA: sinus arteriosus, PVO: posterior ventricular outgrowth). Symbols indicate different populations (Sitka Sound [SS], Prince William Sound [PWS], and Washington [WA]), where red-bordered symbols indicate the doses where PVO areas are significantly different from no-oil controls. All populations show a dose-response (p-values of population-specific dose-response indicated in inset table), but the dose response varied between populations (dose-by-population interaction $p<0.0001$). B: Images of representative 1 dph larvae from the PWS population in each exposure treatment. Images on the right are magnifications of the area surrounding the heart, where yellow dashed, pink dashed, and pink solid lines are drawn around the atrium, ventricle, and PVO, respectively. Asterisks indicate treatments where PVO areas were significantly smaller than controls.

Molecular mechanisms of cardiovascular system development and perturbation by oil exposure

We detected oil-induced differences in gene expression at only 2 dpf which is one day after initiation of exposure, and at the lowest dose tested (13.4 ± 1.6 ng/g wet wt., 0.06 ± 0.004 µg/L). This indicates that biological relevance of exposures starts at the earliest stages of development and at extremely low doses. We did not detect a lowest-observable effect level (LOEL) for transcriptional responses to oil – indeed, the molecular response LOEL for Pacific herring may be below our analytical detection limits for many PAH analytes.

Oil exposure-induced molecular responses were substantial and offer insight into the mechanisms that underlie oil toxicity, including impacts on the developing cardiovascular system. Exposure responses were detected early and at low doses, but transcriptional perturbations were most severe at higher doses and later developmental stages. We first characterized the pattern of normal gene expression through development (with no oil exposure), by grouping genes by timing of peak expression (5 modules of peak expression; Fig. 11A),

where development is characterized by consecutive waves of transient gene expression. We then tested whether any of the five temporal modules were perturbed by oil exposure. The temporal module that normally peaks in expression at 6 dpf was perturbed by oil, where perturbation was most pronounced at 4 dpf (Fig. 11B). This group of genes was enriched for those with molecular functions related to cardiovascular system development and function, such as *cardiac muscle cell*, *muscle contraction*, *muscle cell differentiation*, *heart development*, and *angiogenesis* (Fig. 11C). Since cardiogenesis begins at ~4 dpf in herring, these molecular outcomes are consistent with oil exposure perturbing the earliest stages of heart development. At only 2 dpf, oil exposure-induced molecular functions include *xenobiotic metabolism*, consistent with a defensive response, but also *heart development* and *cardiogenesis*, suggesting that oil-induced cardiovascular dysfunction starts to unfold very early in development and quickly after the beginning of exposure (Fig. 12). Molecular pathways associated with heart development and cardiogenesis are perturbed by oil exposure throughout embryogenesis, whereas pathways associated with muscle contraction and metabolic processes are perturbed by oil in the latter stages of embryonic development (Fig. 12).

Many xenobiotic response genes (34) were differentially expressed upon oil exposure during early through to late stages of embryogenesis. Differentially expressed xenobiotic response genes were primarily Phase 1 metabolism genes (e.g., cytochrome P450s, aldehyde dehydrogenases) or those that control initiation of transcription of Phase 1 xenobiotic metabolism genes (e.g., ahrr and aip). The *xenobiotic metabolism* Kyoto Encyclopedia of Genes and Genomes (KEGG) pathway was significantly enriched among oil exposure perturbed genes at 2, 4, 6, and 10 dpf. Xenobiotic metabolism gene expression varied between developmental time points (Fig. 13), with more genes eliciting a linear dose response to increasing concentrations of ∑PAHs in the middle of embryonic development (4 dpf), at the same time that PAH uptake was rapidly increasing (Fig. 9B). Oil-induced regulation of xenobiotic metabolism genes became less pronounced as embryonic development progressed (e.g., by 8 dpf and 10 dpf) and embryonic capacity to metabolize and excrete xenobiotics increased, leading to lower ∑PAH concentrations by 10 dpf (Fig. 9B). It is apparent that even the earliest stages of embryos are capable of mounting metabolic responses to xenobiotic exposures, which effectively reduced PAH body burdens between 4 dpf and 10 dpf. Unfortunately, even at the very low doses included in our experiment, this defensive response was incapable of protecting against toxicity (e.g., cardiac development), either because xenobiotic metabolism was overwhelmed or because of production of toxic metabolites.

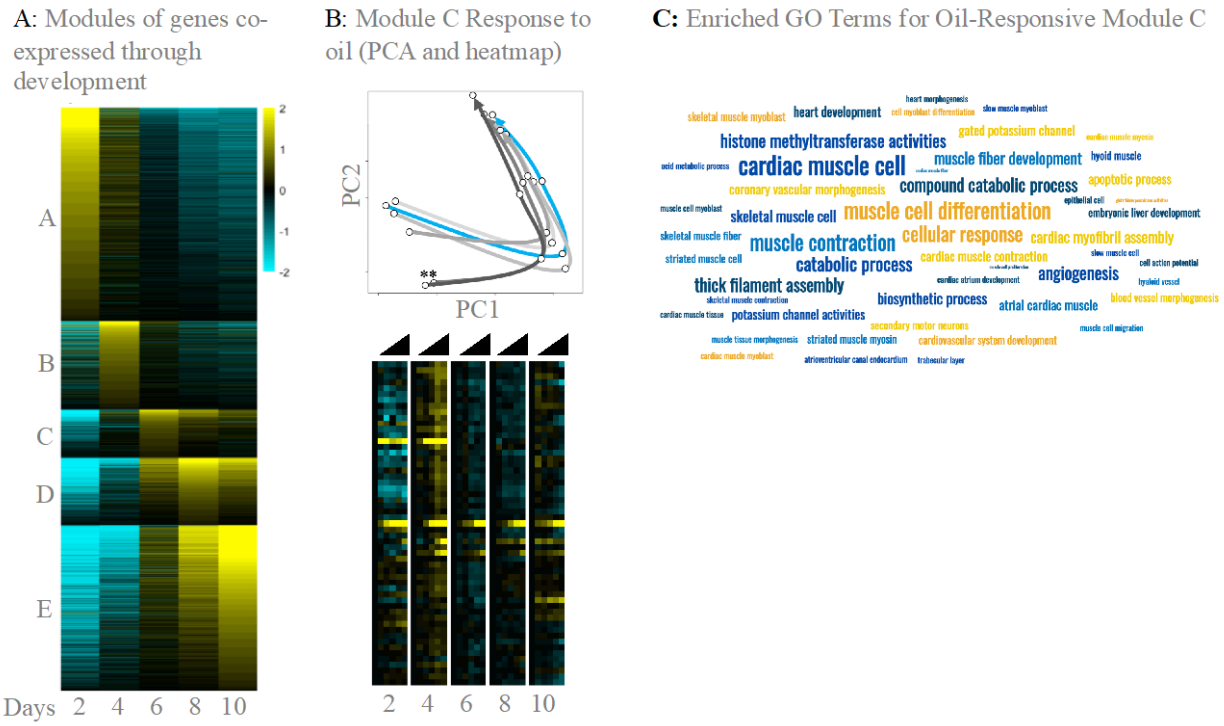

Figure 11. Genome-wide transcriptional change through development and in response to oil exposure. A: Modules (A to E) of genes that are co-expressed during embryogenesis (days 2, 4, 6, 8, and 10 post fertilization), grouped by timing of peak expression. Columns are treatments, rows are genes, and color of cells indicate log2 expression level following normalization to the treatment mean, such that yellow and blue indicate higher or lower expression, respectively, compared to the treatment mean. B: Module C from the heatmap in panel A was perturbed by oil exposure, indicated by principle components analysis plot of Module C genes (top) where arrows indicate the trajectories of transcriptional change through time (early through late development from base to tip of arrow) for each dose (control is blue, and gray through black for increasing oil dosage groups) and asterisks indicate significant dosage deviation, and by heatmap (bottom) where wedges indicate increasing dose and color (log2 expression level) is scaled relative to controls for each day. C: Gene ontology (GO) terms that are statistically significantly enriched in module C that was perturbed by oil exposure, where font size is scaled by effect size (fold-enrichment). Terms with the smallest effect size are cardiac muscle fiber, muscle cell proliferation and glutathionine peroxidase activities.

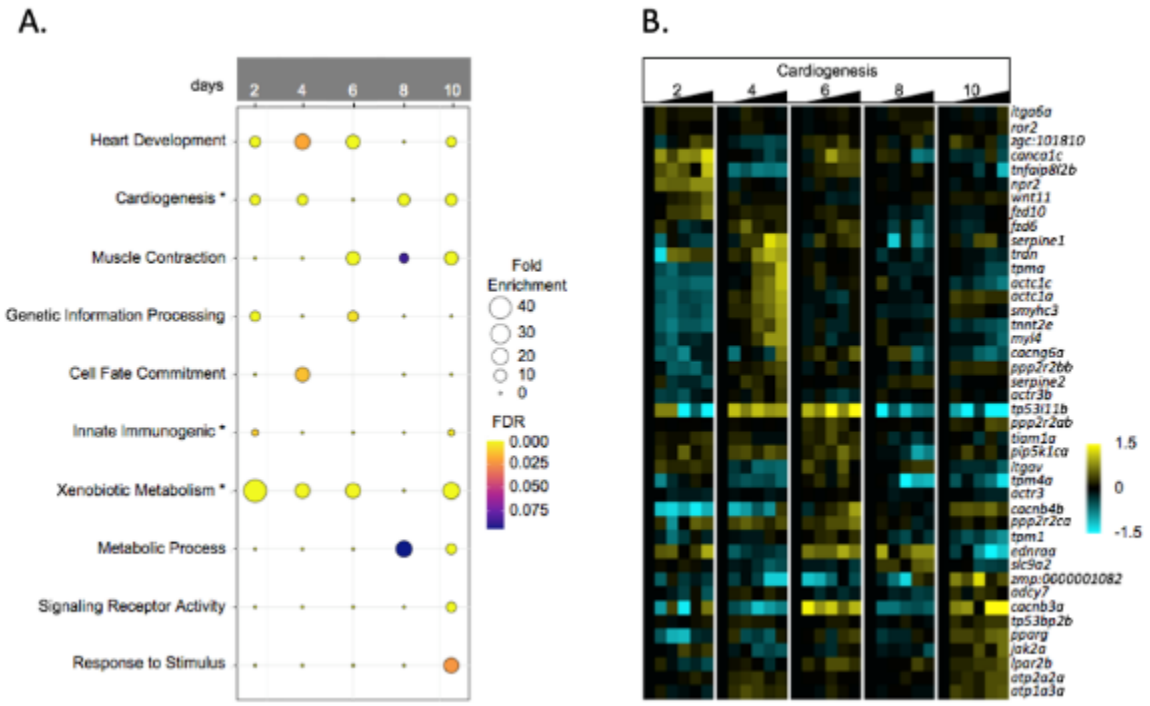

Figure 12. Transcriptional responses to oil exposure throughout development. A: KEGG pathways and manually-curated gene sets (asterisks) that were statistically significantly enriched for transcriptional responses to oil exposure at each day of sampling (columns; 2, 4, 6, 8, and 10 days post-fertilization) through embryogenesis. Colors of circles scale with false discovery rate (FDR) corrected p-value, and sizes of dots scale with fold enrichment (effect size). B: Genes involved in cardiac function and development for which transcription was perturbed by oil exposure. Sets of columns indicate the increasing dose response at each day of development (2, 4, 6, 8, and 10 dpf). Rows indicate log2 expression of genes, where color indicates up-regulation (yellow) or down-regulation (blue) relative to stage-specific controls (black).

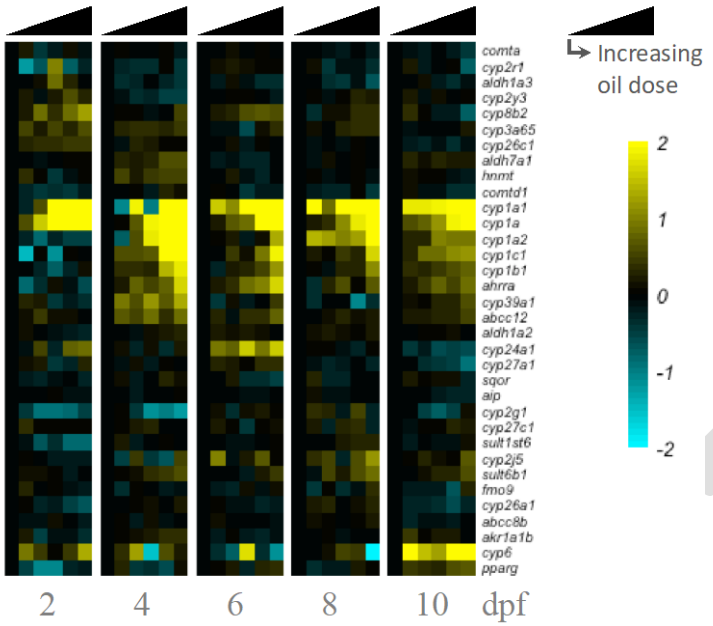

Figure 13. Genes involved in xenobiotic metabolism for which transcription was perturbed by oil exposure. Sets of columns indicate the increasing dose response at each day of development (2, 4, 6, 8, and 10 dpf). Rows indicate log2 expression of genes, where color indicates up-regulation (yellow) or down-regulation (blue) relative to stage-specific no-oil controls (black).

Many oil exposure-induced transcriptional responses were conserved between the three populations (Fig. 14A). At developmental days 4, 6, and 10, the number of transcripts showing a conserved dose response between populations was 16, 19, and 1695, respectively (FDR<0.1). At 4 dpf, genes that are differentially regulated during oil exposure were enriched for the KEGG pathway *Metabolism of Xenobiotics by Cytochrome P450* (p=0.003), including many Phase I and II metabolism genes such as cyp1a1, cyp1b1, cyp1c1, cyp1a2, and ugt1b5. At 6 dpf, the conserved oil dose response was largely characterized by an upregulated transcriptional response of a battery of xenobiotic response genes including cyp1a, cyp1a1, cyp1a2, cyp1c1, cyp1b1, ahrra, ugt1b5, and sult6b1. The conserved dose response at 10 dpf is characterized by significantly greater transcriptional perturbation (1,695 genes) than observed at earlier developmental time-points. The 1,695 genes with a conserved oil dose response were divided into up- and down-regulated genes (726 and 696, respectively) for functional enrichment analysis. There was no significant enrichment for KEGG pathways in 10 dpf up-regulated genes. *Endocytosis*, however, was significantly enriched (p=0.004) in down-regulated genes. The endocytosis pathway is responsible for the transport of exogenous nutrients, proteins and ligand into the cytoplasm. Additional notable conserved up-regulated genes at 10 dpf include those involved in xenobiotic metabolism (cyp1a1, cyp1a2, cyp1c1, cyp1b1, cyp39a1, ahrra, ugt1a1, ugt1b5, and sult6b1). Cardiac genes were abundant but not significantly enriched among those showing a conserved dose-response at 10 dpf.

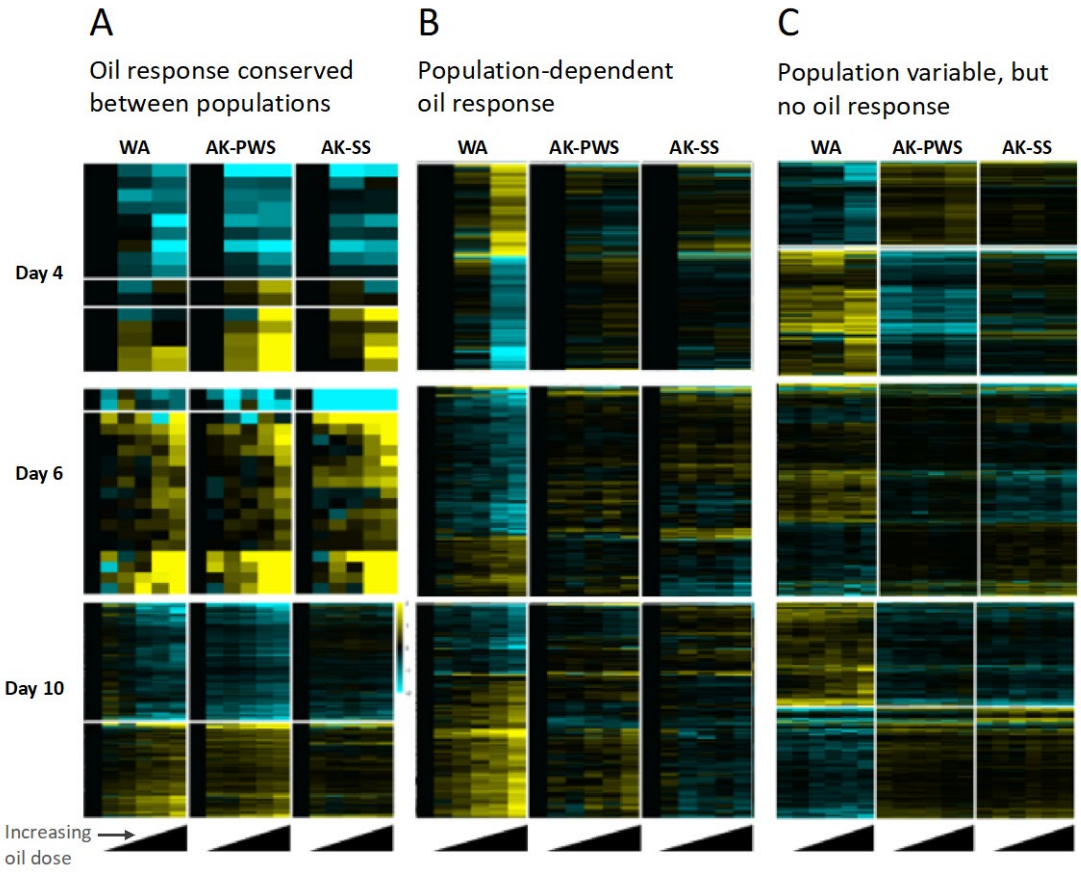

Figure 14. Patterns of population variation in gene expression for Pacific herring from Washington (WA), Prince William Sound (AK-PWS), and Sitka Sound (AK-SS). Sets of columns are increasing doses of oil for each population. Rows indicate log2 expression of genes, where color indicates up-regulation (yellow) or down-regulation (blue) relative to either stage-specific controls for each population (panels A and B; black) or population means (panel C). Transcriptional patterns are grouped by day post-fertilization of development (4, 6, or 10 dpf). A: Genes that were transcriptionally responsive to oil exposure, but that did not vary in their transcriptional response between populations; that is, they were transcriptional responses to oil that were conserved between populations. B: Genes that showed a population-dependent transcriptional response to oil exposure (significant dose-by-population interaction). C: Genes that did not transcriptionally respond to oil, but that varied in expression between populations.

Transcriptional responses to oil varied between populations, where the two Alaska populations (PWS and SS) were most similar, and the WA population was most different (Fig. 14B). This is consistent with population variation in their susceptibility to oil-induced cardiac injury (Fig. 10). Though the number of genes showing a conserved transcriptional response to oil increased with developmental age (Fig. 14A), population-dependent responses showed the reverse pattern where the earliest stage had the most transcriptional responses distinguishing WA fish from the other

populations (Fig. 14B). This suggests that the mechanisms responsible for the reduced toxicity observed in WA fish compared to AK fish included those induced by oil very early in development. The molecular responses to oil that distinguish WA from AK fish at 4 dpf include the KEGG pathway *intestinal immune network for IgA production*. The WA-specific response to oil at 6 dpf is enriched for the KEGG pathway *cardiac muscle contraction*, for our manually curated set of cardiac development and function genes, and for our manually curated set of immune system and function genes. No KEGG pathways were enriched for population-dependent responses to oil at 10 dpf. This pattern of population variation is consistent with our expectations based on random-neutral drift, insofar as the most genetically distinct population (WA) shows the most distinct transcriptional response to oil (Fig. 14B) (Fst between WA and each of the AK populations [0.011 for WA vs. PWS, and 0.0099 for WA vs. SS] is larger than Fst between the two AK populations [0.0088]). This pattern is apparent not only for oil responsive genes, but also for genes that are not transcriptionally responsive to oil; that is, for genes that are only variable between populations (and that do not transcriptionally respond to oil exposure), the WA population is most distinct (Fig. 14C).

Specific characterization of the transcriptional response of a manually curated set of xenobiotic response and metabolism genes (Fig. 15) reveals both conserved (Fig. 15B) and population-dependent (Fig. 15C) responses. More xenobiotic response genes show a conserved transcriptional response to oiling than a population-dependent response. Conserved responses are observed across all developmental timepoints (Fig. 15B), whereas the population-dependent response is primarily observed at 4 dpf (Fig. 15C). The population-dependent responses indicate that the WA population is the outlier compared to the two AK populations (Fig. 15C).

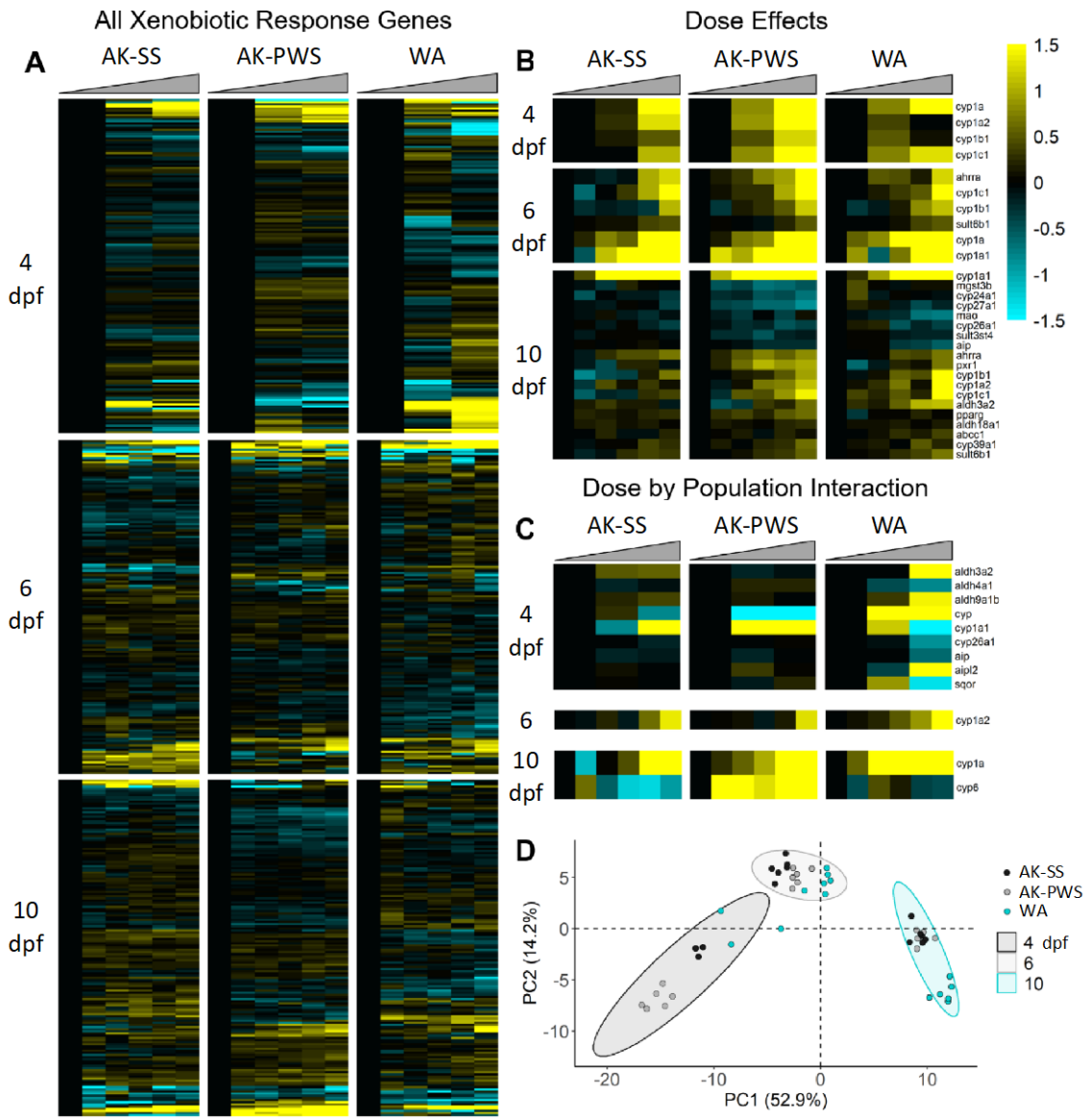

Figure 15. Xenobiotic response genes of herring from Sitka Sound (AK-SS), Prince William Sound (AK-PWS), and Washington (WA) and their transcriptional response to oil exposure. A: All manually-curated xenobiotic response genes, and their expression at each developmental stage sampled (4, 6, and 10 days post fertilization [dpf]; top, middle, and bottom set, respectively), for each population. Wedges at the top of columns indicate increasing dose of oil. Rows indicate log2 expression of genes, where color indicates up-regulation (yellow) or down-regulation (blue) relative to stage-specific controls (black) for each population. B: Xenobiotic response genes that had a statistically significant transcriptional response to oil, where the response was the same in each population. C: Xenobiotic response genes that had a statistically significant transcriptional response to oil, but where the response was different between populations. D: Principal components plot of all xenobiotic metabolism genes for each population (colors) and developmental times (dpf; symbols).

Impacts of brief early-life oil exposure during embryogenesis on juvenile sensitivity to VHSV

VHSV virulence was high, causing 70%-80% mortality over 21 days. This level of virulence did not vary between populations and did not depend on whether fish had been exposed to oil many months before during embryogenesis (Fig. 16A). In a follow-up experiment fish from only the PWS population were briefly exposed to oil during a different stage of early life: as larvae they were exposed to oil for 20 days starting at 2-weeks post-hatch. These fish, and control no-oil exposed fish, were subsequently raised to juvenile stage in clean water then exposed to VHSV. Virulence (mortality) was reduced in fish that had been briefly exposed to oil during early larval development (Fig. 16B). The molecular mechanisms that underlie response to VHSV, including in fish that had been exposed to oil as larvae, are not reported here since analysis is still incomplete, but this work is ongoing.

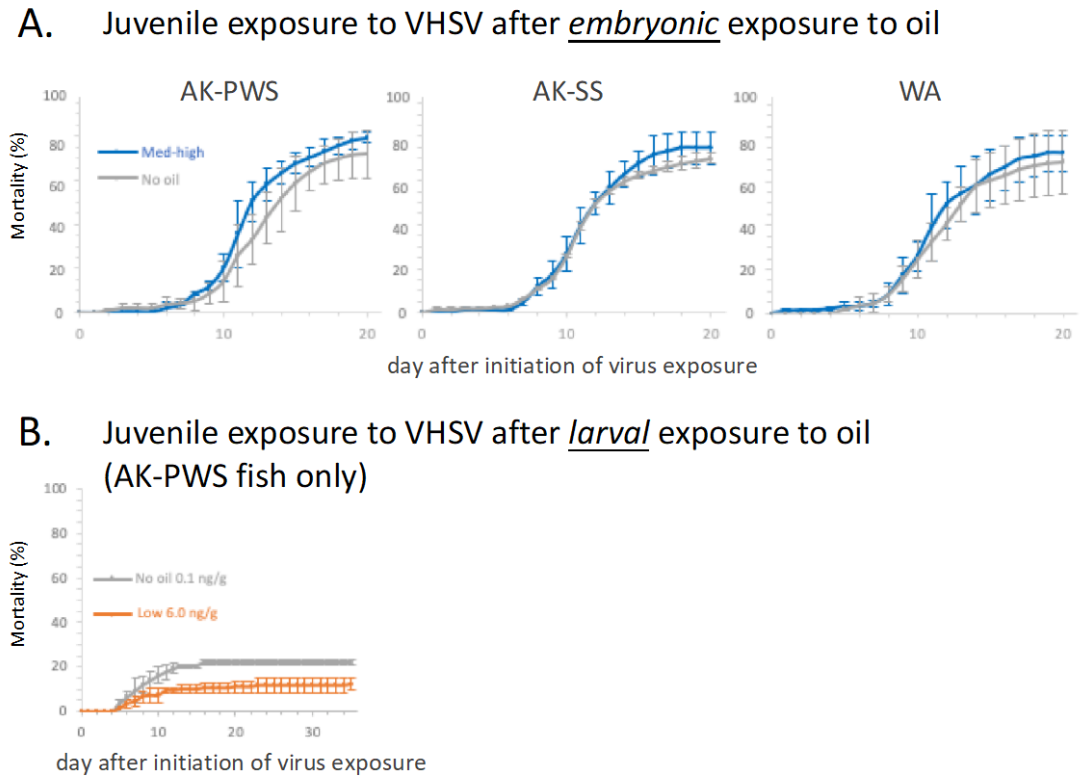

Figure 16. Mortality of post-metamorphosis juvenile Pacific herring in response to viral (VHSV) exposure. A: Mortality for fish from each of three populations (Prince William Sound [AK-PWS], Sitka Sound [AK-SS], and Washington [WA]) for fish that had been exposed to oil during embryogenesis (blue lines) and control fish that had not been exposed to oil (grey lines). B: Mortality for fish from the AK-PWS population that had been exposed to oil as larvae for three weeks starting two-weeks post-hatch (orange line) and controls not exposed to oil (grey line).

Molecular mechanisms of immune system development and perturbation by oil exposure
We established a framework for characterizing innate immune system development by manually curating set of 1,744 genes involved in immune system development and function. We examined the expression of these genes throughout development, from embryogenesis through hatch and later until early-stage juveniles by which time immune system development should be mature (78 dpf) (Fig. 17). After characterizing the transcriptional arc of innate immune system development in Pacific herring, we tested whether oil exposure perturbed the expression of these genes. Transcriptional analysis of the initiation and development of the innate immune system was determined by ordering genes by peak expression across nine time-points (Fig. 17), including five time-points pre-hatch and four time-points after hatch through to juvenile metamorphosis. Visualization of immune gene expression reveals two major developmental clusters representing pre-hatch embryogenesis (2-10 dpf) and post-hatch larval to juvenile stage (1-78 dph) (Fig. 17A). Immune system genes that are highly expressed in embryogenesis tend to reduce expression after hatch. In contrast, most immune system genes are not highly expressed until after hatch, and those genes tend to remain highly expressed through subsequent sampling times (Figure 17B). In teleost fishes the first line of defense against invading pathogens is the physical barrier of the chorion. A week after shedding the protective chorion herring begin feeding, further intensifying interactions between the developing immune system and the environment. In early embryogenesis, overrepresentation analysis of KEGG pathways showed the strongest enrichment at 2 and 4 dpf for the *Wnt*, *FoxO*, *MAPK*, and *MTOR* signaling pathways, which are non-specific multi-functional pathways involved in normal development and organismal growth. In contrast, significantly enriched KEGG pathways post-hatch include *Bacterial Infection*, *MAPK Signaling*, *NOD-like Receptor Signaling*, and the *C-type Lectin Receptor Signaling pathway*, reflecting the maturation of the innate immune system after hatch. Together, these patterns suggest that the onset of innate immune function occurs after hatch and continues into late-larval/early juvenile stages.

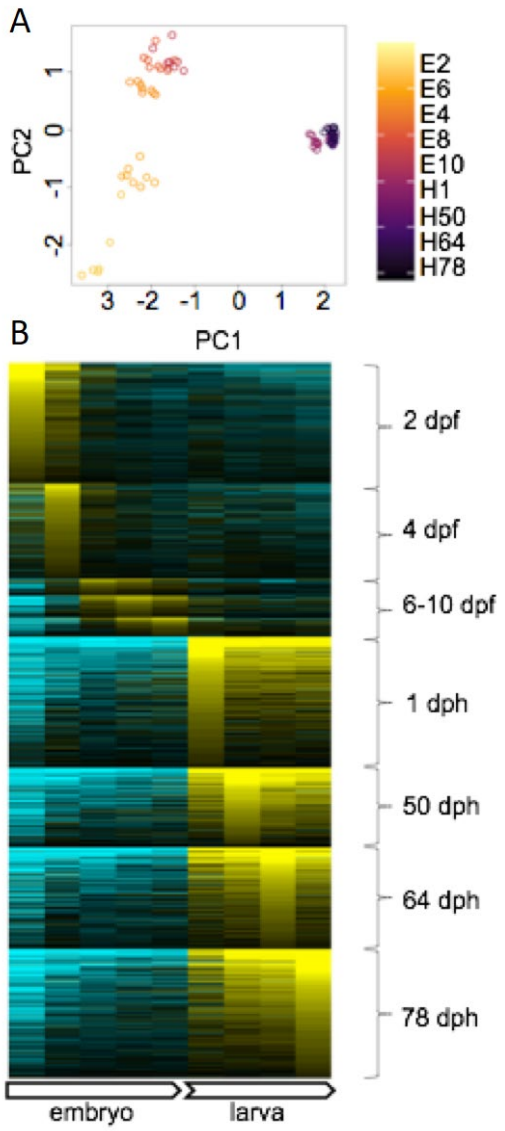

Figure 17. Expression of immune system genes through development. A: Principal components analysis illustrates overall temporal variance in the expression of immune system genes at different developmental stages, where colors indicate embryonic (E) developmental times (2, 4, 6, 8, and 10 days post fertilization [dpf]) and post-hatch larval (H) developmental times (1, 50, 64, and 78 days post hatch [dph]). B: Heatmap for immune system genes, grouped by developmental stage of peak expression. Columns indicate developmental stage, and rows indicate log2 expression of genes, where color indicates up-regulation (yellow) or down-regulation (blue) relative to the mean expression level (black).

Oil exposure had only a subtle impact on immune gene expression. During embryogenesis, our manually curated set of innate immune genes were over-represented in oil-perturbed genes at 2 dpf and 10 dpf (Fig. 12A). Oil perturbed genes at 2 dpf were associated with Wnt and BMP signaling, and protein biogenesis, all of which are involved in growth and development. At 2 dpf,

one gene, itpkcb, was up-regulated in response to the lowest oil dose (13.4 ng/g ∑PAH). This gene is involved in phosphorylation and is normally expressed in the hatching gland of fish embryos, which is located in the pericardium. Genes perturbed by oil by the last day of exposure (10 dpf) include those involved in cytokine signaling. Interestingly, the majority of oil-perturbed immune-related genes at 10 dpf are also associated with the cardiovascular system - particularly the *Apelin Signaling pathway* - suggesting interactions between cardiotoxicity and immunotoxicity. Differential expression analysis revealed almost no genes perturbed by oil in fish sampled post-hatch. Our earliest post-hatch sampling is 1 dph, which was four days after the termination of oil exposure. These subtle and limited perturbations of immune system genes by oil exposure during embryogenesis are consistent with the lack of impact of embryogenic oil exposure on juvenile sensitivity to VSHV exposure. Most immune system genes initiate expression after hatch, which was after our embryonic oil exposure window. Our subsequent oil exposure experiment where exposure was during early larval stages, when many immune system genes are starting to be expressed, and these exposures did modulate later-life sensitivity to VHSV exposure. The molecular mechanisms underlying this immune-modulating larval oil exposure are still under investigation.

DISCUSSION

Aim 1

Population genomics data reveals the genetic structuring of Pacific herring throughout their entire eastern-Pacific range, from the Bering Sea and Gulf of Alaska in the north to San Francisco Bay in the south. The Bering Sea population (TB) is most distinct from all other populations, where measures of genome-wide genetic differentiation compared to other populations are high (Pairwise Fst: 0.125-0.198). This suggests that the Alaska Peninsula has historically served as a stronger barrier to dispersal than the large geographical distance that separates the Gulf of Alaska from California. Alternatively, the Bering Sea environment might require adaptations that are distinct from other parts of the species' range, such that migration is reduced between that region and others. Further analysis of genomic regions showing particularly large differentiation between TB and other populations, especially where they coincide with reduced nucleotide diversity in TB fish, could reveal genes that are adaptive for life in the Bering Sea. Considering the remaining populations (not including TB), the California population is most distinct from the Alaska, British Columbia, and Washington populations.. There are no obvious geographical barriers to dispersal between, for example, California and Washington, that would explain this pattern, though perhaps ocean currents north of California limit migratory exchange with more northern regions. Alternatively, environmental conditions in this most southern part of the species' range, such as high temperatures, might require adaptations that are distinct from other parts of the species' range, such that migration is reduced between California and more northerly regions. Ongoing analyses seek to reveal putatively adaptive genes supporting fitness in this southern extreme of the species' geographic range.

Genetic differentiation among populations in the region between the Gulf of Alaska and Washington is low, indicating historical gene flow across this part of the range. The Gulf of Alaska populations (PWS and SS) harbor some signal of introgression from the Bering Sea population (TB), indicating some historical migration around the Alaska Peninsula. But this introgression is not observed outside the Gulf of Alaska (e.g., in British Columbia or Washington populations), indicating that the extent of this historical gene flow is geographically limited to Alaska.

A few major structural genomic features distinguish the California population from all others. At least two large putative chromosomal inversions appear to be segregating at high frequency in the California population, but only at low frequency in others. Chromosomal inversions that segregate between populations often harbor co-adaptive gene complexes that underlie local adaptations. The large inversion on chromosome 12 is in a nearly identical position as in Atlantic herring (Han et al. 2020), and was likely inherited from the common ancestor of both species. In Atlantic herring this inversion is associated with adaptation to alternate seasonal spawn timing. The functional significance of the inversion in California populations of Pacific herring are currently unknown, but an association with spawn timing that differs from more northern populations is a reasonable hypothesis that merits further testing. Another large putative inversion is detected on chromosome 7. It segregates at high frequency in California fish, intermediate frequency in TB fish, and low frequency in the remaining populations, and does not appear to be present in Atlantic herring. The functional and/or adaptive significance of this inversion is unknown and merits further investigation.

Further analysis of genes showing signatures of natural selection along the latitudinal temperature gradient are ongoing, and will be important for identifying genetic variation that is relevant for adaptation to warm temperatures. Once we identify segregating genetic variation that is important for fitness in different thermal environments, we could track the frequency of those mutations through time in Alaska populations as their environment warms in coming decades. This could be a useful method for testing whether Alaska populations are able to evolve fast enough to keep pace with global climate change.

Estimates of temporal genetic effective population size (Ne) for Alaska populations offer insight into population changes between the early 1990s and 2017 that have affected demography. When allele frequencies genome-wide change little from one time point to another this indicates a weak influence of drift which is observed in large effective population sizes. In contrast, when allele frequencies show greater change through time, this indicates an elevated influence of random genetic drift, which is observed in groups with lower effective population size. In examining allele frequency change between successive sampling times, we calculated very low effective population sizes (high temporal variance). However, for species where census population sizes are very large (like for Pacific herring) and the sample size used to calculate Ne is comparably small (~60 fish per time point in our study), then methods for calculating Ne can be inaccurate (Marandel et al. 2019). We therefore caution the reader to be skeptical of the absolute measures

of Ne that we report here until we explore this in further detail. In contrast, we are more confident in the value of the relative patterns of Ne between and within populations that we detect. Little change in Ne across this period of time for TB and SS populations is consistent with only minor demographic perturbations. In contrast, in the PWS population Ne increases in the decade between 1995 and 2005, then declines over the following decade. This is consistent with significant demographic perturbations in PWS fish during these periods. Additional analysis is required to examine whether these changes in effective population size are consistent with fluctuations in census population sizes over these same time periods.

Outlier-based selection scans through time within each of the Alaska populations did not show a strong influence of natural selection over the time period examined. This result is consistent with what has been observed in other intensively harvested fish, where putatively adaptive phenotypic changes over time were not correlated with genetic outliers. At first glance this is perhaps surprising, until one considers that inter-individual variation for most phenotypic traits is likely underpinned by small-effect variants at many genes (Boyle et al. 2017). In this scenario, subtle changes in allele frequency at many loci enables large changes in phenotype (Barton and Keightley 2002, Messer and Petrov 2013), but these types of subtle genetic change are very difficult to detect with traditional outlier-based selection scan methods. An alternative is to test whether allele frequency change (even very small ones) between adjacent time periods covary with change over successive time periods (Buffalo and Coop 2019). Testing for these patterns genome-wide can reveal the more subtle signatures that natural selection exerts on traits that are highly polygenic.

Selection scans based using temporal covariance methods reveal signatures of polygenic selection over time in the PWS population, but not in the other two Alaska populations. This suggests that environmental changes in the PWS habitat in the decades following the EVOS, VHSV epidemic, and population collapse, exerted genotype-specific fitness impacts on PWS fish. Positive temporal covariances were detected in the first two periods (1991-1996 vs. 1996-2006) and in the second two periods (1996-2006 vs. 2006-2017). But this signal disappeared when comparing across both the first and second periods together (1991-1996 vs. 2006-2017). This suggests that selection was influential in each of the two periods, but that selection in the first period affected different genes than in the second period. That is, the selective regime operating in the first period was different that that operating in the second period. The shift in selective regimes over time may be a result of changing environmental conditions over time, such as oil spill toxicity, disease, predation, competition, or warming. One way to generate hypotheses about the traits that are under selection is to examine the identity of genes that are present in selected genomic regions, and test whether these genes are enriched for any particular biological function. In the first period (1991-1996 vs. 1996-2006) we detected significant enrichment of genes involved in *C-C chemokine receptor activity*. This is conspicuous since this is the period over which VHSV swept through the PWS population, and C-C chemokine receptors are important for immune system signaling. Chemokines play a major role in

inflammatory reactions and innate immunity. Importantly, chemokines are specifically induced by exposure to VHSV when examined in various fish models (Sanchez et al. 2007, Chaves-Pozo et al. 2010, Montero et al. 2011, Aquilino et al. 2014, Castro et al. 2014, Kim et al. 2018). Our ongoing studies will reveal if these genes are activated by VHSV exposure in Pacific herring. These findings promote the hypothesis that the VHSV viral epidemic that swept through the PWS population in the 1990's was a selective force leading to evolutionary changes in the innate immune system in PWS fish. Though contemporary PWS fish do not vary in their sensitivity to acute mortality induced by laboratory exposure to VHSV (Fig. 16A), responses that are more subtle than acute lethality may be relevant and important, such that this hypothesis merits further study.

Aims 2 and 3

For animal exposure experiments, our range of ∑PAH concentrations captured the majority of the range of ∑PAH detected in PWS following the spill in 1989 and 1990. Median and mean estimated ∑PAH concentrations in intertidal PWS water in the sampling that followed the spill in 1989 (estimated from PAH residues in indigenous intertidal mussels at oiled shores) was 0.24 µg/L and 0.30 µg/L, respectively (Boehm et al. 2007), which is between our medium-low and medium concentrations (0.15 and 0.53 µg/L), and the arithmetic mean from 1989 sampling was 3.4 µg/L, which matches our high concentration (3.42 µg/L). We therefore conclude that our laboratory experiments provided a useful simulation of the oil exposure severity that occurred in impacted nearshore PWS environments following the 1989 spill event. Our lowest observable effect concentration for cardiovascular developmental toxicity (medium concentration: 0.53 µg/L) was lower than the mean concentration (3.4 µg/L) but slightly higher than the median concentration (0.30 µg/L) estimated in nearshore PWS waters following the 1989 spill (Boehm et al. 2007).

Despite needing to stagger the exposures of different populations at different times (because of variation in the spawn timing of natural populations) our oil dispersion system was able to replicate nearly identical exposure conditions; our dose range was highly similar for the experiment that included the two Alaska populations, and similar to the Washington population exposure which was conducted one month later. We therefore conclude that population responses to oil exposure are comparable because exposure conditions were nearly identical. Although oil concentration ranges were highly similar between populations, oil accumulation in tissues varied between populations. Embryos from the Washington population harbored a different profile of PAH analytes compared to the Alaska populations, indicating population variation in PAH metabolism. Variation in metabolism is supported by gene expression data, where a set of xenobiotic metabolism genes exhibit different transcriptional responses to oiling in the Washington population compared to the Alaska populations. To distinguish whether these differences in PAH metabolism in Washington fish are a function of random neutral drift, or alternatively caused by natural selection, would require contrasts with other Washington (or other nearby) populations.

Transcriptomic responses, across a broad range of doses and across a detailed time series, offer nuanced insight into the molecular mechanisms of action that follow exposure to crude oil through sensitive early-life developmental stages. We are still analyzing this broad and deep dataset to detail the developmental time-course of molecular perturbations that connect oil exposures to cardiovascular dysfunction. Molecular responses to oil were apparent at the lowest dose and at the earliest stage of development. This suggests that even trace levels of oil exposure are bioavailable and elicit biological responses. These responses are nearly immediate – within one day following the initiation of exposure. Surprisingly, the very earliest responses were detected in embryos as young as 2 dpf. This suite of immediate/early responsive genes included mostly Phase I and II metabolism genes, indicating that a metabolic defensive response to oil can be inducible in very early life. This metabolism response likely accounted for the unusual temporal profile of PAH body burdens, where PAHs accumulate up to 4 dpf then decrease by 10 dpf, despite constant concentrations in the surrounding water.

Populations of Pacific herring varied in their response to oil exposure. Parallel dose-responses were observed in the two Alaska populations (PWS and SS), but the Washington population diverged. Total PAH body burdens in Washington population fish by 10 dpf was slightly lower than in Alaska fish, despite water concentrations being highly consistent. WA fish were also less sensitive to the cardiac developmental malformations caused by exposures, insofar as higher body burdens of ∑PAH were required to cause similar levels of cardiac developmental impairment in Washington fish compared to Alaska fish. We conclude that the oil spill exposure history in the PWS population has not sensitized or de-sensitized PWS fish to the toxicity of oil, at least compared to the other Alaska population (SS). We designed our three-population contrasts to expose whether divergent responses in Alaska populations were best explained by neutral or adaptive processes. Instead of variation between Alaska populations, we found that the Washington population was most different in their response to oil. Since the Washington population is most different in background genetics compared to the Alaska populations, we cannot distinguish whether their divergent response to oil is because of random neutral drift, or whether natural selection - perhaps in response to pollution in Puget Sound - has played a role. Different population contrasts, that include other populations from Washington or nearby, would be necessary to test this hypothesis.

Molecular responses to oil exposure that distinguish Washington fish from Alaska fish offer insight into the mechanisms that contribute to reduced sensitivity of Washington fish to oil-induced cardiovascular developmental perturbation. Xenobiotic metabolism genes show a different response to oil in the Washington fish compared to Alaska fish, especially in early development (4 dpf). This may be responsible for the shift in PAH body burden profiles observed by 10 dpf in Washington fish compared to Alaska fish, and for reduced cardiovascular developmental perturbation in larval Washington fish compared to Alaska fish. Although differential metabolism may contribute to reduced sensitivity of Washington fish to oil, it is not likely to be entirely responsible, because even at similar body burdens Washington fish appear

less sensitive to oil-induced cardiac endpoints. We find that genes involved in cardiovascular development and function are differentially expressed in response to oil in Washington fish compared to Alaska fish, especially at 6 dpf, which is a critical phase of development for the cardiovascular system. We conclude that differential metabolism of xenobiotics, coupled with differential sensitivity to oil-induced perturbation of cardiovascular development pathways, contribute to the reduced sensitivity to cardiovascular injury observed in Washington fish in response to oil exposure compared to Alaska fish.

Oil exposure during embryogenesis did not affect juvenile sensitivity to VHSV-induced mortality, nor did populations vary in their sensitivity to VHSV. This is consistent with early-life exposure to oil not affecting later-life sensitivity to virus. However, it is premature to accept that conclusion. That is because most immune system maturation occurs after hatch (Fig. 17), which was several days after the termination of oil exposure in our experiments. Therefore, it is plausible that oil exposure may impair immune system development and maturation, but that we did not expose fish during a consequential period of immune development. Indeed, our exposures started two weeks post-hatch, which is when key components of the immune system are coming online, and did affect later-life sensitivity to oil (Figure 16B). Additional experiments, with exposures that coincide with different periods of immune development (e.g., the first two weeks post-hatch), or that span longer periods of development (embryogenesis to late-larval), are necessary to provide for definitive conclusions about the impacts of early-life oil exposure on later-life immune competency. Similarly, our data indicate no population variation in their response to VHSV, which supports the conclusion that historical oil exposures and epizootics did not cause evolved differences in PWS fish. However, this conclusion is also premature. We compared population sensitivity to VHSV-induced mortality which did not differ, whereas other physiological consequences of VHSV-induced morbidity may vary between populations. Furthermore, our experiments only tested for population variation in their innate immune response to VHSV, whereas subsequent exposures that engage the adaptive immune response may expose population differences. Finally, we tested population variation in response to only one strain of VHSV; populations may vary in their response to other VHSV strains, and in their response to other pathogens. Additional experiments are required to test these hypotheses. These additional experiments may be especially merited given that genes involved in key components of the immune system response in fish (cytokine signaling genes) appear to have been the targets of polygenic adaptive evolution in PWS fish over the past three decades following the spill and VHSV epizootic.

CONCLUSIONS

Patterns of genetic change within populations over the past three decades since the EVOS indicate that natural selection has been influential in the PWS population over this time period, but less influential in other Alaska populations (TB and SS). This suggests that environmental change that has been unique to PWS over this time period has posed fitness challenges for

resident fish, prompting adaptive shifts in many genes. The most obvious environmental changes over this time period that are unique to PWS are the EVOS and VHSV epizootic. In the face of the population crash that followed in the early 1990s, the influence of natural selection is evident against the background signal of genetic drift. Ongoing investigations are identifying the functions of genes within the regions of the genome that appear adaptive in PWS fish, such that they may inform the attributes of those fish that have been under selection, and thereby illuminate the drivers of fitness challenges over this consequential time period. Preliminary results reveal cytokine receptor genes enriched in those adaptive regions of the genome, which are involved in immune responses to virus. This is consistent with VHSV acting as a force for evolutionary change in PWS, but this hypothesis requires further experiments. Although mortality in response to acute VHSV exposure did not vary between populations, ongoing data analyses are testing whether the molecular/cellular responses of PWS fish to VHSV challenge are different from other populations, which would add further evidence of relevance to this hypothesis. We detected a shift in selective regimes that split the first and second half of the time period examined. This is consistent with complex and dynamic environmental change in PWS over the past three decades that has been consequential for the fitness of PWS herring. Across the broader range of North American populations, we detect large structural mutations – putative chromosomal inversions – that are segregating within and between populations. Most of these are enriched at high frequency in the California population, and at least one appears shared with Atlantic herring. The function of these inversions, and the ecological reasons for their enrichment in California fish, are the subject of ongoing investigation.

Oil exposures caused molecular perturbations at the lowest exposure concentrations, and at the earliest life stages, consistent with the exquisite sensitivity of developing fish to crude oil toxicity. The effective concentrations were well within the range detected in PWS in 1989 and 1990, such that similar responses and injuries were likely experienced by PWS fish during spawning in those years. Molecular data are offering detailed insight into the mechanisms that underlie xenobiotic defense responses, cardiovascular developmental impairment, and immune system developmental impairment in response to oil exposure and mechanisms that underlie physiological responses to VHSV challenge. Comparisons between populations (PWS, SS, and WA) in their physiological responses to oil challenge and VHSV challenge do not indicate that PWS fish are distinct in their response. Washington fish appear most distinct from the two Alaska populations – they are least sensitive to the cardiovascular developmental impacts of oil. Since Washington fish are the most genetically distinct from the three (most distant shared ancestry), these differences cannot be attributed to either the influence of neutral drift or local adaptation and requires additional population contrasts.

Oil exposure during embryogenesis did not affect later-life sensitivity to oil. However, since immune system development does not appear to mature until after hatch, especially immediately after hatch, perhaps oil exposure during early larval stages would impact immune development and later-life sensitivity to virus – additional experiments are required to test this hypothesis. In

support of this hypothesis, we found that oil exposure starting two weeks after hatch did affect later-life sensitivity to virus. Exposures that span the complete time period of immune system maturation, especially during the first two weeks after hatch, are required to complete our understanding of how oil exposure during early life may or may not cause perturbations to immune system development, which may then persist to later life and affect sensitivity to pathogen challenge.

ACKNOWLEDGEMENTS

Archived frozen tissue samples from Prince William Sound (PWS) and Sitka Sound (SS) populations prior to 2017 were contributed from the collection maintained by the Alaska Department of Fish and Game (ADF&G). Collections director Chris Habicht and staff members Judy Berger and Heather Hoyt facilitated the selection and transfer of tissues from their collection to the University of California Davis. In 2017 Sherri Dressel and Katie Sechrist (ADF&G) arranged for collection of fresh tissue samples from Togiak Bay fish in coordination with Ben Cain at Silver Bay Seafoods (Bristol Bay/Naknek plant). 2017 samples from PWS and SS were collected by Ashley Mackenzie (Hershberger group, U. S. Geological Survey). Outside of Alaska, tissues were collected in 2017 from central British Columbia (Canada) arranged by Kristen Daniel and Jaclyn Cleary (Department of Fisheries and Oceans Canada), from Puget Sound by Tiffany Linbo (Scholz/Incardona group, National Oceanic and Atmospheric Administration), and from San Francisco Bay arranged by Kathy Hieb (California Department of Fish and Wildlife). Additional funding support was contributed by the SeaDoc Society. This project is part of the Herring Research and Monitoring program. These findings and conclusions presented by the author are their own and do not necessarily reflect the views or position of the *Exxon Valdez* Oil Spill Trustee Council.

LITERATURE CITED

Alberti, M. 2015. Eco-evolutionary dynamics in an urbanizing planet. Trends in Ecology & Evolution 30:114–126.

Aquilino, C., R. Castro, U. Fischer, and C. Tafalla. 2014. Transcriptomic responses in rainbow trout gills upon infection with viral hemorrhagic septicemia virus (VHSV). Developmental & Comparative Immunology 44:12–20.

Barton, N. H., and P. D. Keightley. 2002. Understanding quantitative genetic variation. Nature Reviews. Genetics 3:11–21.

Boehm, P. D., J. M. Neff, and D. S. Page. 2007. Assessment of polycyclic aromatic hydrocarbon exposure in the waters of Prince William Sound after the *Exxon Valdez* oil spill: 1989–2005. Marine Pollution Bulletin 54:339–356.

Bolger, A. M., M. Lohse, and B. Usadel. 2014. Trimmomatic: a flexible trimmer for Illumina sequence data. Bioinformatics 30:2114–20.

Boyle, E. A., Y. I. Li, and J. K. Pritchard. 2017. An expanded view of complex traits: from polygenic to omnigenic. Cell 169:1177–1186.

Buffalo, V., and G. Coop. 2019. The linked selection signature of rapid adaptation in temporal genomic data. Genetics 213:1007–1045.

Buffalo, V., and G. Coop. 2020. Estimating the genome-wide contribution of selection to temporal allele frequency change. Proceedings of the National Academy of Sciences 117:20672–20680.

Carls, M. G., G. D. Marty, and J. E. Hose. 2002. Synthesis of the toxicological impacts of the *Exxon Valdez* oil spill on Pacific herring (*Clupea pallasi*) in Prince William Sound, Alaska, USA. Canadian Journal of Fisheries and Aquatic Sciences 59:153–172.

Castro, R., B. Abós, J. Pignatelli, L. von G. Jørgensen, A. G. Granja, K. Buchmann, and C. Tafalla. 2014. Early Immune Responses in Rainbow Trout Liver upon Viral Hemorrhagic Septicemia Virus (VHSV) Infection. PLOS ONE 9:e111084.

Chang, C. C., C. C. Chow, L. C. Tellier, S. Vattikuti, S. M. Purcell, and J. J. Lee. 2015. Second-generation PLINK: rising to the challenge of larger and richer datasets. GigaScience 4:s13742-015-0047–8.

Chaves-Pozo, E., J. Montero, A. Cuesta, and C. Tafalla. 2010. Viral hemorrhagic septicemia and infectious pancreatic necrosis viruses replicate differently in rainbow trout gonad and induce different chemokine transcription profiles. Developmental & Comparative Immunology 34:648–658.

Cherr, G. N., E. Fairbairn, and A. Whitehead. 2017. Impacts of Petroleum-Derived Pollutants on Fish Development. Annual Review of Animal Biosciences, Vol 5:185–203.

Cingolani, P., A. Platts, L. L. Wang, M. Coon, T. Nguyen, L. Wang, S. J. Land, X. Lu, and D. M. Ruden. 2012. A program for annotating and predicting the effects of single nucleotide polymorphisms, SnpEff. Fly 6:80–92.

Ewels, P., M. Magnusson, S. Lundin, and M. Käller. 2016. MultiQC: summarize analysis results for multiple tools and samples in a single report. Bioinformatics 32:3047–3048.

Fukuyama, A. K., G. Shigenaka, and R. Z. Hoff. 2000. Effects of residual Exxon Valdez oil on Intertidal *Protothaca staminea*: Mortality, growth, and bioaccumulation of hydrocarbons in transplanted clams. Marine Pollution Bulletin 40:1042–1050.

Fumagalli, M., F. G. Vieira, T. Linderoth, and R. Nielsen. 2014. ngsTools: methods for population genetics analyses from next-generation sequencing data. Bioinformatics 30:1486–1487.

Garcia-Erill, G., and A. Albrechtsen. 2020. Evaluation of model fit of inferred admixture proportions. Molecular Ecology Resources 20:936–949.

Gassmann, A. J., Y. Carriere, and B. E. Tabashnik. 2009. Fitness Costs of insect resistance to *Bacillus thuringiensis*. Annual Review of Entomology 54:147–163.

Ge, S. X., D. Jung, and R. Yao. 2020. ShinyGO: a graphical gene-set enrichment tool for animals and plants. Bioinformatics (Oxford, England) 36:2628–2629.

Griffin, F. J., M. C. Pillai, C. A. Vines, J. Kääriä, T. Hibbard-Robbins, R. Yanagimachi, and G. N. Cherr. 1998. Effects of salinity on sperm motility, Fertilization, and development in the Pacific herring, *Clupea pallasi*. The Biological Bulletin 194:25–35.

Han, F., M. Jamsandekar, M. E. Pettersson, L. Su, A. P. Fuentes-Pardo, B. W. Davis, D. Bekkevold, F. Berg, M. Casini, G. Dahle, E. D. Farrell, A. Folkvord, and L. Andersson. 2020. Ecological adaptation in Atlantic herring is associated with large shifts in allele frequencies at hundreds of loci. eLife 9:e61076.

Hendry, A. P., T. J. Farrugia, and M. T. Kinnison. 2008. Human influences on rates of phenotypic change in wild animal populations. Molecular Ecology 17:20–29.

Hershberger, P. K., M. K. Purcell, L. M. Hart, J. L. Gregg, R. L. Thompson, K. A. Garver, and J. R. Winton. 2013. Influence of temperature on viral hemorrhagic septicemia (Genogroup IVa) in Pacific herring, Clupea pallasii Valenciennes. Journal of Experimental Marine Biology and Ecology. Volume 444.

Hicken, C. E., T. L. Linbo, D. H. Baldwin, M. L. Willis, M. S. Myers, L. Holland, M. Larsen, M. S. Stekoll, S. D. Rice, T. K. Collier, N. L. Scholz, and J. P. Incardona. 2011. Sublethal exposure to crude oil during embryonic development alters cardiac morphology and reduces aerobic capacity in adult fish. Proceedings of the National Academy of Sciences.

Hochmuth, J. D., L. De Meester, C. M. S. Pereira, C. R. Janssen, and K. A. C. De Schamphelaere. 2015. Rapid adaptation of a *Daphnia magna* population to metal stress Is associated with heterozygote excess. Environmental Science & Technology 49:9298–9307.

Incardona, J. P., M. G. Carls, L. Holland, T. L. Linbo, D. H. Baldwin, M. S. Myers, K. A. Peck, M. Tagal, S. D. Rice, and N. L. Scholz. 2015. Very low embryonic crude oil exposures cause lasting cardiac defects in salmon and herring. Scientific Reports 5:13499.

Kim, K.-H., W.-J. Kim, C.-J. Park, J.-W. Park, G. E. Noh, S. Lee, Y. M. Lee, and H. C. Kim. 2018. Analysis of manifestation of CC and CXC chemokine genes in olive flounders (*Paralichthys olivaceus*) artificially infected with VHSV during the early developmental stage. Development & Reproduction 22:341–350.

Kolde, R. 2012. Pheatmap: pretty heatmaps. R package version 1:726.

Kopelman, N. M., J. Mayzel, M. Jakobsson, N. A. Rosenberg, and I. Mayrose. 2015. Clumpak: a program for identifying clustering modes and packaging population structure inferences across K. Molecular Ecology Resources 15:1179–1191.

Korneliussen, T. S., A. Albrechtsen, and R. Nielsen. 2014. ANGSD: analysis of next generation sequencing data. Bmc Bioinformatics 15:356.

Korunes, K. L., and K. Samuk. 2021. pixy: Unbiased estimation of nucleotide diversity and divergence in the presence of missing data. Molecular Ecology Resources 21:1359–1368.

Law, C. W., Y. Chen, W. Shi, and G. K. Smyth. 2014. voom: precision weights unlock linear model analysis tools for RNA-seq read counts. Genome Biology 15:R29.

Li, H. 2011. A statistical framework for SNP calling, mutation discovery, association mapping and population genetical parameter estimation from sequencing data. Bioinformatics 27:2987–2993.

Li, H., and R. Durbin. 2009. Fast and accurate short read alignment with Burrows–Wheeler transform. Bioinformatics 25:1754–1760.

Marandel, F., P. Lorance, O. Berthelé, V. M. Trenkel, R. S. Waples, and J.-B. Lamy. 2019. Estimating effective population size of large marine populations, is it feasible? Fish and Fisheries 20:189–198.

Martin, M. 2011. Cutadapt removes adapter sequences from high-throughput sequencing reads. EMBnet.journal 17:10–12.

Marty, G. D., P.-J. F. Hulson, S. E. Miller, T. J. Quinn, S. D. Moffitt, and R. A. Merizon. 2010. Failure of population recovery in relation to disease in Pacific herring. Diseases of Aquatic Organisms 90:1–14.

Marty, G. D., T. J. Q. II, G. Carpenter, T. R. Meyers, and N. H. Willits. 2003. Role of disease in abundance of a Pacific herring (*Clupea pallasi*) population. Canadian Journal of Fisheries and Aquatic Sciences 60:1258–1265.

Meisner, J., and A. Albrechtsen. 2018. Inferring population structure and admixture proportions in low-depth NGS data. Genetics 210:719–731.

Messer, P. W., and D. A. Petrov. 2013. Population genomics of rapid adaptation by soft selective sweeps. Trends in Ecology and Evolution 28:659–669.

Monosson, E. 2012. Evolution in a Toxic World : How Life Responds to Chemical Threats. Island Press, Washington, DC.

Montero, J., J. Garcia, M. C. Ordas, I. Casanova, A. Gonzalez, A. Villena, J. Coll, and C. Tafalla. 2011. Specific regulation of the chemokine response to viral hemorrhagic septicemia virus at the entry site. Journal of Virology 85:4046–4056.

National Research Council. 2007. Toxicity Testing in the 21st Century: A Vision and a Strategy. The National Academies Press, Washington, DC.

Nordtug, T., A. J. Olsen, D. Altin, S. Meier, I. Overrein, B. H. Hansen, and Ø. Johansen. 2011. Method for generating parameterized ecotoxicity data of dispersed oil for use in environmental modelling. Marine Pollution Bulletin 62:2106–2113.

Oziolor, E. M., N. M. Reid, S. Yair, K. M. Lee, S. Guberman VerPloeg, P. C. Bruns, J. R. Shaw, A. Whitehead, and C. W. Matson. 2019. Adaptive introgression enables evolutionary rescue from extreme environmental pollution. Science 364:455–457.

Patro, R., G. Duggal, M. I. Love, R. A. Irizarry, and C. Kingsford. 2017. Salmon provides fast and bias-aware quantification of transcript expression. Nature Methods 14:417–419.

Pearson, W. H., R. A. Elston, R. W. Bienert, A. S. Drum, and L. D. Antrim. 1999. Why did the Prince William Sound, Alaska, Pacific herring (*Clupea pallasi*) fisheries collapse in 1993 and 1994? Review of hypotheses. Canadian Journal of Fisheries and Aquatic Sciences 56:711–737.

Pettersson, M. E., C. M. Rochus, F. Han, J. Chen, J. Hill, O. Wallerman, G. Fan, X. Hong, Q. Xu, H. Zhang, S. Liu, X. Liu, L. Haggerty, T. Hunt, F. J. Martin, P. Flicek, I. Bunikis, A. Folkvord, and L. Andersson. 2019. A chromosome-level assembly of the Atlantic herring genome-detection of a supergene and other signals of selection. Genome Research 29:1919–1928.

Pinsky, M. L., A. M. Eikeset, C. Helmerson, I. R. Bradbury, P. Bentzen, C. Morris, A. T. Gondek-Wyrozemska, H. T. Baalsrud, M. S. O. Brieuc, O. S. Kjesbu, J. A. Godiksen, J. M. I. Barth, M. Matschiner, N. Chr. Stenseth, K. S. Jakobsen, S. Jentoft, and B. Star. 2021. Genomic stability through time despite decades of exploitation in cod on both sides of the Atlantic. Proceedings of the National Academy of Sciences 118:e2025453118.

Poplin, R., V. Ruano-Rubio, M. A. DePristo, T. J. Fennell, M. O. Carneiro, G. A. V. der Auwera, D. E. Kling, L. D. Gauthier, A. Levy-Moonshine, D. Roazen, K. Shakir, J. Thibault, S. Chandran, C. Whelan, M. Lek, S. Gabriel, M. J. Daly, B. Neale, D. G. MacArthur, and E. Banks. 2018. Scaling accurate genetic variant discovery to tens of thousands of samples. bioRxiv. <https://www.biorxiv.org/content/10.1101/201178v3>. Accessed 2 Jan 2023.

Purcell, S., B. Neale, K. Todd-Brown, L. Thomas, M. A. R. Ferreira, D. Bender, J. Maller, P. Sklar, P. I. W. de Bakker, M. J. Daly, and P. C. Sham. 2007. PLINK: A tool set for whole-genome association and population-based linkage analyses. American Journal of Human Genetics 81:559–575.

Qi, Q., M. Toll-Riera, K. Heilbron, G. M. Preston, and R. C. MacLean. 2016. The genomic basis of adaptation to the fitness cost of rifampicin resistance in Pseudomonas aeruginosa. Proceedings of the Royal Society B: Biological Sciences 283:20152452.

Reid, N. M., D. A. Proestou, B. W. Clark, W. C. Warren, J. K. Colbourne, J. R. Shaw, S. I. Karchner, M. E. Hahn, D. Nacci, M. F. Oleksiak, D. L. Crawford, and A. Whitehead. 2016. The genomic landscape of rapid repeated evolutionary adaptation to toxic pollution in wild fish. Science 354:1305–1308.

Reynaud, S., and P. Deschaux. 2006. The effects of polycyclic aromatic hydrocarbons on the immune system of fish: A review. Aquatic Toxicology 77:229–238.

Ritchie, M. E., B. Phipson, D. Wu, Y. Hu, C. W. Law, W. Shi, and G. K. Smyth. 2015. limma powers differential expression analyses for RNA-sequencing and microarray studies. Nucleic Acids Research 43:e47.

Robinson, M. D., and A. Oshlack. 2010. A scaling normalization method for differential expression analysis of RNA-seq data. Genome Biology 11:R25.

Sanchez, E., J. Coll, and C. Tafalla. 2007. Expression of inducible CC chemokines in rainbow trout (Oncorhynchus mykiss) in response to a viral haemorrhagic septicemia virus (VHSV) DNA vaccine and interleukin 8. Developmental & Comparative Immunology 31:916–926.

Short, J. W., G. V. Irvine, D. H. Mann, J. M. Maselko, J. J. Pella, M. R. Lindeberg, J. R. Payne, W. B. Driskell, and S. D. Rice. 2007. Slightly weathered Exxon Valdez oil persists in Gulf of Alaska beach sediments after 16 years. Environmental Science & Technology 41:1245–50.

Short, J. W., M. R. Lindeberg, P. M. Harris, J. M. Maselko, J. J. Pella, and S. D. Rice. 2004. Estimate of oil persisting on the beaches of Prince William Sound 12 years after the Exxon Valdez oil spill. Environmental Science & Technology 38:19–25.

Short, J. W., J. M. Maselko, M. R. Lindeberg, P. M. Harris, and S. D. Rice. 2006. Vertical Distribution and Probability of Encountering Intertidal Exxon Valdez Oil on Shorelines of Three Embayments within Prince William Sound, Alaska. Environmental Science & Technology 40:3723–3729.

Simão, F. A., R. M. Waterhouse, P. Ioannidis, E. V. Kriventseva, and E. M. Zdobnov. 2015. BUSCO: assessing genome assembly and annotation completeness with single-copy orthologs. Bioinformatics 31:3210–3212.

Skotte, L., T. S. Korneliussen, and A. Albrechtsen. 2013. Estimating individual admixture proportions from next generation sequencing data. Genetics 195:693–702.

Sloan, C. A., B. F. Anulacion, K. A. Baugh, J. L. Bolton, D. Boyd, R. H. Boyer, D. G. Burrows, D. P. Herman, R. (Ronald) Pearce, and G. M. Ylitalo. 2014. Northwest Fisheries Science Center's analyses of tissue, sediment, and water samples for organic contaminants by gas chromatography/mass spectrometry and analyses of tissue for lipid classes by thin layer chromatography/flame ionization detection. Northwest Fisheries Science Center (U.S.) and N. O. and A. A. United States, editors. <https://repository.library.noaa.gov/view/noaa/4626>.

Soneson, C., M. I. Love, and M. D. Robinson. 2015. Differential analyses for RNA-seq: transcript-level estimates improve gene-level inferences. F1000Research 4:1521.

Sørensen, L., M. S. Silva, A. M. Booth, and S. Meier. 2016. Optimization and comparison of miniaturized extraction techniques for PAHs from crude oil exposed Atlantic cod and haddock eggs. Analytical and Bioanalytical Chemistry 408:1023–1032.

Therkildsen, N. O., and S. R. Palumbi. 2017. Practical low-coverage genomewide sequencing of hundreds of individually barcoded samples for population and evolutionary genomics in nonmodel species. Molecular Ecology Resources 17:194–208.

Thorne, R. E., and G. L. Thomas. 2008. Herring and the "Exxon Valdez" oil spill: an investigation into historical data conflicts. ICES Journal of Marine Science 65:44–50.

Townsley, B. T., M. F. Covington, Y. Ichihashi, K. Zumstein, and N. R. Sinha. 2015. BrAD-seq: Breath Adapter Directional sequencing: a streamlined, ultra-simple and fast library preparation protocol for strand specific mRNA library construction. Frontiers in Plant Science 6. <https://www.frontiersin.org/articles/10.3389/fpls.2015.00366>. Accessed 2 Jan 2023.

Trochta, J. T., T. A. Branch, A. O. Shelton, and D. E. Hay. 2020. The highs and lows of herring: A meta-analysis of patterns and factors in herring collapse and recovery. Fish and Fisheries 21:639–662.

Whitehead, A. 2013. Interactions between Oil-Spill Pollutants and Natural Stressors Can Compound Ecotoxicological Effects. Integrative and Comparative Biology 53: 635-647.

Wingett, S. W., and S. Andrews. 2018. FastQ Screen: A tool for multi-genome mapping and quality control. F1000Research 7:1338.

OTHER REFERENCES

Peer reviewed publications

Oziolor, E. M., N. M. Reid, S. Yair, K. M. Lee, S. Guberman VerPloeg, P. C. Bruns, J. R. Shaw, A. **Whitehead***, and C. W. Matson*. 2019. Adaptive introgression enables evolutionary rescue from extreme environmental pollution. Science. 364: 455-457. (* co-corresponding authors). *Note: though research reported in the above publication does not include Pacific herring data, it did use methods and analyses that our group developed for our EVOSTC funded Pacific herring research. We therefore cite the EVOSTC funding in the acknowledgements for this paper.*

Reports

Whitehead, A. 2018. Genomic mechanisms that underlie lack of recovery of Prince William Sound herring following the 1990's collapse. Annual Report, Project 17170115. *Exxon Valdez* Oil Spill Trustee Council, Anchorage, Alaska. https://evostc.state.ak.us/media/2137/2017-17170115-annual.pdf

Whitehead, A. 2019. Genomic mechanisms that underlie lack of recovery of Prince William Sound herring following the 1990's collapse. Annual Report,Project 18170115. *Exxon Valdez* Oil Spill Trustee Council, Anchorage, Alaska. https://evostc.state.ak.us/media/2139/2018-18170115-annual.pdf

Whitehead, A. 2020. Genomic mechanisms that underlie lack of recovery of Prince William Sound herring following the 1990's collapse. Annual Report, (Project 19170115. *Exxon Valdez* Oil Spill Trustee Council, Anchorage, Alaska. https://evostc.state.ak.us/media/7117/19170115-annual-report.pdf

Whitehead, A. 2021. Genomic mechanisms that underlie lack of recovery of Prince William Sound herring following the 1990's collapse. Annual Report, Project 20170115. *Exxon Valdez* Oil Spill Trustee Council, Anchorage, Alaska. https://evostc.state.ak.us/media/7487/20120115-annual-report.pdf

Publicly available datasets

Whitehead, A. 2022. Population genomics of Pacific herring across space (from California to Alaska) and through time (for Alaska populations from 1991 to 2017): NCBI BioProject

submission: SUB4072937 (https://submit.ncbi.nlm.nih.gov/subs/bioproject/SUB4072937/overview).

Tisthammer, K., J. McGirr, and A. **Whitehead**. 2022. Computational/bioinformatic scripts for population genomics analyses. https://github.com/joemcgirr/pac_herring, https://github.com/kahot/PacHerring.

Scientific Presentations

Gill, T., T. Linbo, P. Hershberger, J. Incardona, and A. **Whitehead**. 2019. Interactions between oil exposure and immune function relevant for Pacific herring population collapse. Poster Presentation. Annual Meeting of the Society of Environmental Toxicology and Chemistry. Toronto, Ontario, Canada. November.

Outreach

Hershberger, P., T. Gill, and A. **Whitehead**. 2020. From oil slick to chronically sick? Delta Sound Connections 2020-2021. Prince William Sound Science Center. https://pwssc.org/wp-content/uploads/2020/07/DSC-2020-web.pdf